Design of hundered gram Femtosatellite made from commercially available parts

Syed Aamir Ali Naqvi

School of Electrical Engineering

Thesis submitted for examination for the degree of Master of Science in Technology.

Espoo 11.4.2017

Thesis supervisor:

Prof. Jaan Praks

Aalto University
School of Electrical
Engineering

AALTO UNIVERSITY
SCHOOL OF ELECTRICAL ENGINEERING

ABSTRACT OF THE
MASTER'S THESIS

Author: Syed Aamir Ali Naqvi

Title: Design of hundered gram Femtosatellite made from commercially available parts

Date: 11.4.2017 Language: English Number of pages: 8+69

Department of Electronics and Nanoengineering

Professorship: Space Science and Technology (S-92)

Supervisor and advisor: Prof. Jaan Praks

The topic of this thesis is femtosatellite, a new class of spacecraft with a mass of only a hundred grams. The goal of the work is to evaluate the feasibility of a femtosatellite made from commercially available subsystems and components. To achieve this goal, a femtosatellite is designed based on careful analysis of every subsystem in the small satellite.

Different options for various subsystems are presented, and selection between suitable subsystems is performed. Moreover, some parts of the satellite are designed during this work. For example, a circular patch antenna is designed with Computer Simulated Technology (CST) software manufactured by Microwave Studio software suite. The satellite design is based on a commercially available Raspberry Pi Zero computer and the payload of the satellite is an optical camera.

For the system, a careful analysis is performed with regarding the link budget, energy budget, and mass budget. Moreover, the operational scenarios are simulated to assure the ability of the satellite to send and receive images taken from LEO orbit.

The work also gives an overview of previous designs and studies carried out on femtosatellite concepts and compares them to larger satellites in terms of cost, structure, and also functionality.

Keywords: Satellite, Femtosatelite and Space Technology

Preface

I discovered the topic for my thesis when one friend of mine Syed Hasnain Tanveer Kazmi suggested it to me. I immediately realized that I could take this project with the knowledge that I already possess and the great faculty that we have in Aalto University.

I want to start by thanking the supervisor of this thesis, Associate Professor Jaan Praks for accepting the topic of this thesis, his overall good guidance and especially his patience, motivation and good knowledge for this thesis.

I also wish to thank Dr. Jari Holopainen and my fellow colleagues, Nemanja Jovanovic, Riwanto Bagus and Petri Niemalä for their constant help, guidance and useful conversations during the process of researching and writing the thesis.

Last but not least, I would like to express my heartfelt thanks to my Mother and my Father Mr. and Mrs. Syed Zahoor ul Hasnain Shah for their ceaseless blessings, love, and support. I would also like to thank my brothers and my friends for always being there for me.

Above all, I would like to thank God Almighty, for his blessings and support during my studies.

Otaniemi, 14.9.2017

Syed Aamir Ali Naqvi

Contents

Abstract ii

Preface iii

Contents iv

Symbols and abbreviations vi

1 Introduction 1

2 Background 5

3 Femtosatellite Mission and Design 7
3.1 Design Process . . . 8

4 Power Subsystem 10
4.1 Solar Panels . . . 10
4.2 Charge Controller . . . 13
4.3 Battery . . . 14

5 Antenna Subsystem 18
5.1 Background of Circular Patch Antenna . . . 19
5.2 Design and Simulation of Circular Patch Antenna with Air Gap in CST 21
5.3 Radiation Pattern of the Circular Patch Antenna . . . 26
5.4 Return Loss or S11 Parameter . . . 28

6 Communication Subsystem 30
6.1 Link Budget of the Satellite . . . 30
6.2 Communication System Design . . . 31
6.3 Communication Chip Layout . . . 33
6.4 Power Amplifier . . . 36
6.5 Low Noise Amplifier . . . 37

7 Attitude Control of satellite 41
7.1 Attitude Control Design . . . 42

8 On Board Computer(OBC) 45
8.1 On-Board Computer Design . . . 45

9 Payload 48
9.1 Camera Payload . . . 49

10 Structure of Satellite 52
10.1 Commercially Available Structure . . . 52

11 Internal Design of Femtosatellite **56**
11.1 Block Diagram 56
11.2 Schematic 57
11.3 Mass and Power Budget 58

12 Conclusions **61**

13 Summary **62**

References **63**

Symbols and abbreviations

Symbols

Latin Symbols

A	Ampere
Ag	Silver
Al	Aluminum
Ant	Antenna
Au	Gold
B	Magnetic Flux Density
Cu	Copper
d	Distance of Horizon
f	Frequency
Fe	Iron
G	Gravitational Constant
h	Height
m_E	Mass of Earth
Ni	Nickle
r	Radius of Earth
R	Distance
v	Velocity

K	Boltzmann Constant
Pt	Tranmitting Antenna Power
Pr	Power of Receiving Antenna
Gt	Gain of Transmitting Antenna
Gr	Gain of Receiving Antenna
Pn	Noise Power

Greek Symbols

ϵ	Permittivity
ϵ_r	Relative Permittivity
λ	Wavelength
ω	Circular Frequency
μ	Permeability

Abbreviations

Al_2O_3	Aluminium Oxide
ACS	Attitude Control System
ADCS	Attitude Determination And Control System
ASU	Arizona State University
C_5	Five Hour Discharge Time
CE0 and CE1	Chip Selects
CMOS	Complementary Metal Oxide Semiconductor
CSI	Camera Serial Interface
CST	Computer Simulated Technology
DEVM	Dynamic Error Vector Magnitude
EIRP	Effective or Equivalent Isotropic Radiated Power
EO	Earth Observation
EOL	End of Life
FIFO	First in First out
EPS	Electric Power System
FE	Finite Elements
FSK	Frequency Shift Keying
GaInP	Gallium Indium Phosphide
GaAs	Gallium Arsenide
Ge	Germanium
GFSK	Gaussian Frequency Shift Keying
GPS	Global Positioning System
GPIO	General purpose Input Output
HDMI	High Definition Media Interface
HT	High Throughput
I2C	Integrated Circuit (Multiple chips connectable)
IGRF	International Geomagnetic Reference Field
Iop	Optimal Output Current
ISS	International Space Station
ITAR	International Traffic in Arms Regulations
JST	Japanese Solderless Terminal
LNA	Low Noise Amplifier
LED	Light Emitting Diode
LEO	Lower Earth Orbit
LIPO	Lithium Ion Polymer
MCS	Modulation and Coding Set
MCU	Microcontroller Unit
MEMS	Micro Electro Mechanical System
MISO	Master Input Slave Output
MOSI	Master Output Slave Input
MPPT	Maximum Power Point Tracking

Abbreviations

OBC	On Board Computer
OBSW	On Board Software
P	Pixel
PA	Power Amplifier
PDET	Power Detector
pHEMT	Pseudomorphic High Electron Mobility Transistor
POUT	Output Power
Pr	Power Of The Receiver
PSRR	Power Supply Rejection Ratio
PSSCT	Pico-Satellite Solar Cell Test Bed
RH	Relative Humidity
RF	Radio Frequency
SCLK	Serial Clock
S/C	Spacecraft
SPI	Serial Peripheral Interface
TASC	Triangular Advanced Solar Cells
TEM	Transverse Eletromagnetic
TM	Transverse Magnetic
TM^z	Transverse Magnetic(Propagating in z Direction)
TiO	Titanium Oxide
Tx	Transmission mode
U	Unit
UART	Universal Asynchronous Receiver-Transmitter
UHF	Ultra High Frequency
UQFN	Ultrathin Quad Flat No-Leads
USB	Universal Serial Bus
UVS	Ultra-Violet Spectrometer
VHT	Very High Throughput
Vop	Optimal Output Voltage
ZIM	Zero Index Metamaterial

1 Introduction

According to Merriam-Webster dictionary, a satellite is "a celestial body that orbits around another larger one." However, making a satellite that can communicate with the Earth has been a difficult task, because satellite making is a tedious and laborious task and even marred by the component cost. High component is because the satellite industry is lucrative and is hindered by high production and launch costs [1].

Even with a ready-to-launch satellite, there exists a possibility, that the rocket could explode and destroy the high-cost satellite. An example, a satellite co-leased by Facebook and intended to bring internet access to parts of sub-Saharan Africa, was destroyed at the launchpad in Florida on 1st of September 2016, when the rocket, which was meant to carry it to space unexpectedly exploded [1].

For decades, the cost of building satellites and sending them to orbit has only been affordable for big governmental institutions. Universities, which were making satellites, depended on federal institutions or companies for funding. For instance, 75% of the U.S. satellite manufacturing revenues come from the U.S. government contracts [2].

Another one of the difficulties in the satellite industry is that one has to acquire different parts from various countries of the world. Buying hardware is difficult because the imports are often restricted by law, for example, the International Traffic in Arms Regulations (ITAR) in the U.S. Such regulations prohibit the export of both space technology and related information to other countries and also restrict the access of non-US individuals to such technologies [3].

The solution to these difficulties lies in technological progress. With the technological progress, satellite parts are becoming more advanced and smaller in size, which has led to both in a reduction of weight and size of satellites. A recent example of such satellites is the QB50 project. The QB50 is the project of an international network of CubeSats for multi-point, proper position measurements in the lower thermosphere and re-entry research. [4].

Projects like the QB50 highlight the usefulness of smaller satellites when compared to the older generation of satellites, which are significantly larger. Such projects also serve as an example for future satellites. The Table 1 and the Figure 1 shows the classification of satellites.

Both the below-given table and Figure 1 provide an effective means for classification of satellites by mass. Although decreasing the size and mass of the satellite reduces the manufacturing time and cost, it also poses many challenges. These challenges include the inability to accommodate large solar panels, therefore limiting the energy capturing and storage capabilities of the satellite, as well as limiting high bandwidth communications through smaller antennas.

On the other hand advantage of these small satellites is not only limited to cost reduction, they can have several different applications depending on mission objectives. One such possibility of it is the launch of a swarm of satellites; desired due to their ease of manufacturing and launch, and covering more area while fewer resources consumed.

Further comparison between satellite classes can be made through its applications.

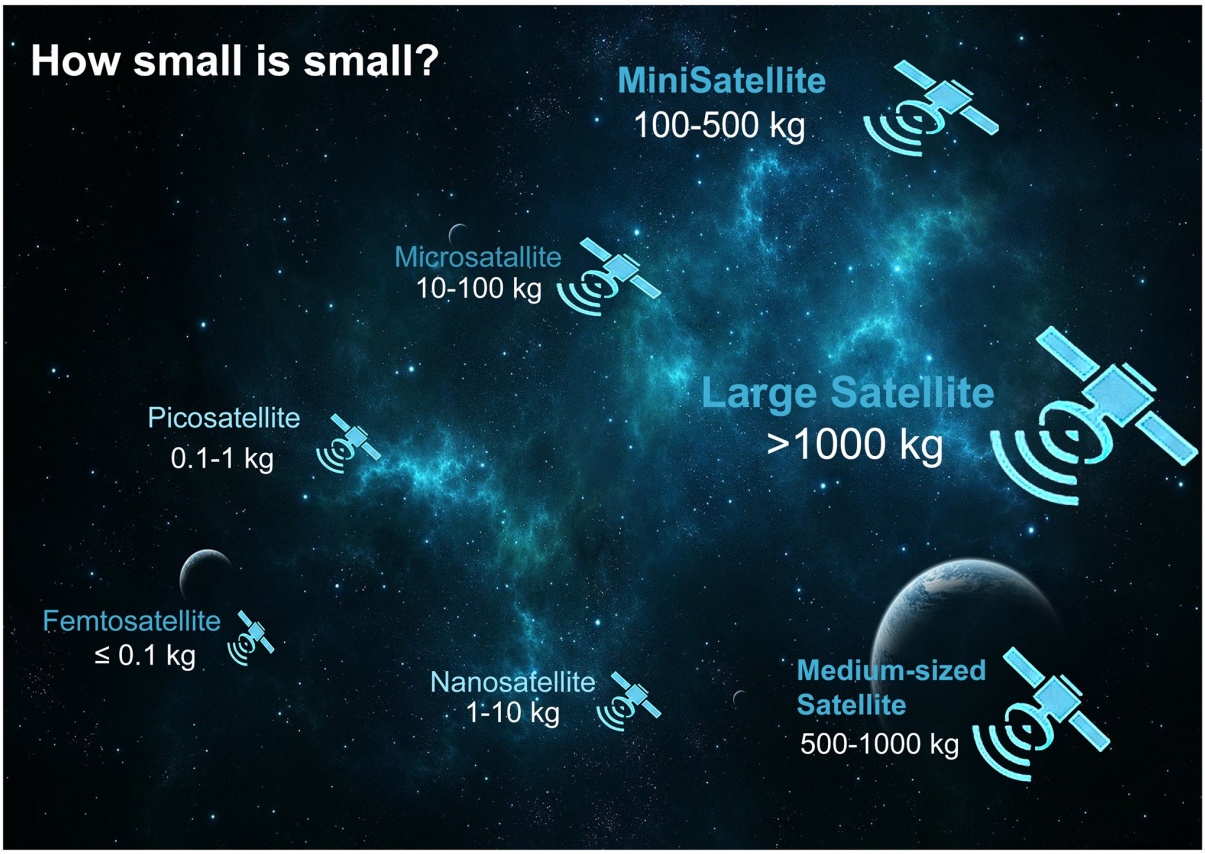

Figure 1: The difference in satellites regarding the mass of the satellites.

For example, analyzing space weather is essential for all kinds of satellites, i.e., those from the civil, governmental and commercial sectors. This analysis is done by larger satellites in size, which measure and analyze space weather by providing information on solar flares.

On the topic of space weather, the femtosatellites which are the smallest class of satellites up-till yet, they can be used in the field of ionospheric research. This concept was first presented in 2008 and later updated in 2012. The research concept was aimed at locating formations of plasma bubbles in the ionosphere, that can deflect signals between the satellites and the ground [5].

The femtosatellite is an innovative technology concept conceived for achieving specific applications with smallest size and mass possible. There are many ways in which this technology is used i.e., the swarm of satellites. The possible advantage of swarm satellites over larger satellites is their ability to map the earth and seaquake damages and provide continuous monitoring of these events from the satellite.

The femtosatellite can be produced and launched for earthquake mapping [6]. This project can be achieved in short time and can be of significant advantage to under-developed countries.

Multiple functions can be performed with the help of a swarm of satellites acting as distributed sensors; for instance, to accurately map the magnetic field of the Earth,

Table 1: Classification for satellites [3]

Satellite class	Wet mass	Example
Large satellite	greater than 1000 kg	
Medium satellite	500 to 1000 kg	GMP
Mini satellite	100 to 500 kg	MiniSat400
Micro satellite	10 to 100 kg	MiniSat100
Nano satellite	1 to 10 kg	SNAP
Small satellites		
Pico satellite	0.1 to 1 kg	CubeSAT
femtosatellite	<=100 g	WikiSat

model Earth's gravitational field or to record meteor showers. This measurement can be done if satellites have sufficient distance between them and they are present in enough numbers. Things such as these can be of significant benefit to the research done by academic institutions.

One more instance through which a comparison can be made, is the drag in Lower Earth Orbit (LEO). Atmospheric drag is caused by repeated collisions of gas molecules with the satellite at orbital altitude. It is one of the leading causes of orbital decay for satellites at LEO. This decay results in the reduction in the altitude of a satellite's orbit.

In LEO the drag in the upper atmosphere is difficult to predict due to its high density and diverse nature [5]. Drag force acts on different satellites and spacecrafts flying in the space environment. This force has impact on spacecraft in LEO [7]. This drag has caused the loss of communication, due to change of position of spacecraft, with different satellites in the pico-satellite solar cell test bed(PSSCT) [5]. The PSSCT program is designed for rapid space environment testing of the next generation solar cells, including measuring IV curves, in space [8]. The communication loss was due to solar activity which stirred a change in the upper atmospheric density at the 400 km altitude, resulting in an increased drag, which caused an immediate change in the position of the spacecraft of 5 degrees [5].

One solution for this drag problem is to have massively distributed femtosatellites in the LEO which could sample atmospheric drag and detect such anomalies, in a cost-effective way.

Apart from this solution for atmospheric drag, femtosatellites also can be used to measure the condition of, and the damages to, larger satellites. The nearby surroundings of large satellites like the ISS (International Space Station) can be checked. Moreover, femtosatellites can continuously monitor the situation of space junk to help devise strategies for reducing it. Femtosatellites can also be used in missions like the Venus Express and the Rosetta Comet mission, where they could be catapulted by the primary satellite to observe different areas of the comet and also the primary satellite itself.

Based on these arguments, the goal of the thesis was derived. The thesis aims to

evaluate the feasibility of the femtosatellite technology, that is, femtosatelite, and especially their ability to communicate from the intended orbit to the ground station. A general payload for this satellite can be represented by a camera. Therefore it would be helpful to know whether the satellite will be able to send data, in the form of images, back to Earth.

The thesis starts by making a background study of femtosatellites, followed by a thorough explanation of the goals of the thesis. After that, the reference design of a femtosatellite is proposed, and it is evaluated subsystem by subsystem. Finally, the conclusions are drawn based on the presented evidence.

2 Background

This background study presents analyses and discusses the technologies that concern femtosatellites, and their functionalities. This background study aims to identify solutions that allow the implementation of femtosatellite technology and presents its possible applications.

This background starts by defining the reasons for the inception of femtosatellite technology. The femtosatellite technology arise from a evolving space industry, as the space industry has moved towards an approach that uses fewer resources to achieve more, the price of getting into space during the 1980s and 1990s led some manufacturers to start making smaller satellites for the different missions, creating the class of "small satellites." Since then, the miniaturization of the spacecraft has been enhanced by further developments in computing and electronics [9].

The enhancements, i.e., the new miniature technologies like CMOS (Complementary Metal-oxide Semiconductor) and MEMS (Micro Electro Mechanical System) allow the development of small processors and systems by using a minimal surface area. These small systems offer the benefit of lowered production costs [10].

Technologies like these, by offering smaller subsystems, have led engineers and researchers to develop lower costing and smaller satellites like Pico and femtosatellites. Picosatellites have become a new alternative to the larger satellites. Current, picosatellites are commercially available across the full range of 0.1–1 kg. Launch opportunities are now available for $12000 to $18000 for sub-1 kg picosatellite payloads, which are about the size of a can of soda [11].

The picosatellite represents an advanced technology, but this technique poses some challenges too, for example, not all of these satellites are successful. Some of the recent launches of picosatellites have been unsuccessful, and only approximately 30 % have shown good results [12].

Further to tackle those challenges, advances in the picosatellite technology has directed the engineers and researchers on to developing an even smaller satellite, i.e., the femtosatellite technology, which requires less time to market, smaller area, simpler architecture, and low power requirement. Moreover, the funding required to produce these satellites has dropped significantly in change from pico to femto.

The Figure 2 shows how much reduction in the five areas pointed in the figure, can be achieved by moving towards femtosatellite technology, and it depicts almost three times the difference between the two satellite types in those five areas.

Another area where femtosatellite excels from picosatellite is coordinated operation of massively distributed femtosatellites. This new class of distributed space missions is rising which needs to have hundreds to thousands of satellites for multi-point, distributed, real-time sensing to achieve much needed Earth observation, remote sensing and science objectives [13].

The low cost, being a significant advantage of this type of satellite, can be seen in all its subsystems, from the low cost of production and equipment to low launching cost. The launch cost, for instance, to be as low as 1000 dollars to orbit near ISS and 3000 dollars to reach Lower Earth Orbit for the launching of a femtosatellite [14].

However, a limited amount of work has been done on femtosatellites, and it brings

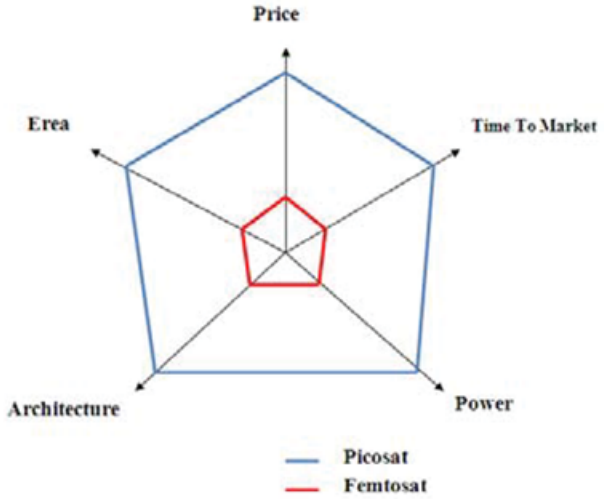

Figure 2: Comparison between pico and femto [12].

exciting new opportunities to the researchers.

These opportunities are in the form of many applications ranging from forecasting, monitoring different areas of Earth, to exploring electron density and magnetic field abnormalities in different orbits. They can be used in projects for various universities and schools but also can have benefits for the military, governmental and private organizations, as they are attractive for both universities and different industries [15].

The standard size for a femtosatellite of 100 g is about 9 cm $\times$ 3 cm $\times$ 3 cm for a three-unit Femtosatellite, which is published on ASU (Arizona State University) website [16]. The size for only one-unit of a femtosatellite is three cm$\times$ 3 cm$\times$ 3 cm for which the weight is 35 g [16].

The design of femtosatellite includes many crucial functional parts, called subsystems. These subsystems can be mentioned as power supply subsystem, communication subsystem, structure subsystem, attitude determination subsystem, orbit determination subsystem, attitude control subsystem and payloads (such as a video recording camera).

3 Femtosatellite Mission and Design

Usually, a satellite has a specified mission which is defined by mission goals. Without a mission, a satellite would have nothing to achieve. This kind of mission also implies which subsystems are inside the femtosatellite.

The purpose of the work is to check whether a femtosatellite, that is made from commercially available parts, can communicate effectively with the ground station. The test of receiving of images on demand is set as the mission of this femtosatellite. The images would be taken with an onboard camera. Therefore, the camera of the femtosatellite is selected as the payload. Transmission of images from the satellite shall test the communication rate, and help to identify difficulties that arise from it. A suitable orbit for taking pictures should be selected.

The research questions are as follows:

- Is a satellite, which is not more than 100 grams, possible to build using commercial subsystems?
- Is this satellite able to communicate from the intended orbit around the Earth?
- What orbit would be suitable for carrying out an EO (Earth observation) mission?
- What type of structure would be appropriate for this type of satellite?
- How much power is needed and what are the sources available to attain this level of power?
- What kind of communication system could be used, and, what type of antenna is feasible for this satellite?
- What kind of attitude subsystem could be used in this satellite?
- What type of on-board computer system is best for this satellite?
- What are the potential application areas of the femtosatellite?

3.1 Design Process

The literature review on this topic includes the work done by Arizona State University (ASU) students [16]. They made a 33 gram 1-U (standard unit) femtosatellite and also presented the design of a 3-U femtosatellite. In thesis of Joshua Tristancho [3], he described all the subsystems of the femtosatellite in detail.

This thesis work was planned to be implemented in different phases. The first step was to define the mission goal and derive requirements for the satellite. Based on previous studies, it was simple to choose a small camera as a payload to evaluate the potential functionality of this femtosatellite.

After the mission of the project was defined, the orbit of this femtosatellite was decided. In both studies [3] [14], the orbit defined for the femtosatellite was LEO (Low Earth Orbit). This is because the further the satellite is from Earth, the more power it will need to communicate with the similar ground station. For more power, large solar panels would be needed which is not possible for femtosatellite.

After the orbit was chosen, the feasibility study was made at this time to know whether the satellite was technically feasible and whether it will be able to communicate to the ground station, within the given weight limit, and from the chosen orbit. Therefore, the link budget, mass and power budgets were made, to investigate the feasibility of those respective subsystems, in order to find out the feasibility of the whole femtosatellite.

After the link and mass budgets, an antenna was designed, which is suited to the link budget of the femtosatellite. The antenna was given main priority because the communication of satellite depends on it. The antenna had to have enough gain, and it should fit to weight limit. This antenna was designed in Computer Simulated Technology (CST) software.

After the antenna was designed in CST, the next task was to design a communication and computing system for the satellite. The primary requirements for these are the same as other subsystems in the project, i.e., they should be a low power and have a low weight to be suitable for the femtosatellite.

The communication subsystem includes a transceiver, a power amplifier, and a low noise amplifier. They all had to have the same frequency range as the antenna, all had to be under the required weight limit, and all were chosen from commercially available parts.

The central computer or the onboard computer of the femtosatellite was chosen according to the requirements, without going into the additional complications of designing it. A computing subsystem was chosen which contains all the connection ports for all the subsystems of the femtosatellite.

The power subsystem was designed from commercially available parts according to the requirement of the power and mass budget. The design process included a selection of solar cells, battery, and a regulator. All components were selected on the basis of the calculated required power of the femtosatellite.

In the end, the focus was on attitude determination and control and the structure of the satellite. For the attitude control subsystem, the decision for choosing an active or passive control was made, which is discussed later in the chapter that deals

with this issue.

For the structure and design of the femtosatellite, it was made according to the design of the antenna and the design of the computer board, so that it encloses them and shields them from any hazardous temperature. In the coming chapters, the designs of all the subsystems are discussed.

4 Power Subsystem

The power supply of the femtosatellite is the source of power for communication, onboard data processing, for attitude control and determination, and for payload.

All the systems need a sufficient amount of power, but small satellite by default, stores and produces the small amount of power, lowering power usage for such a satellite is the main challenge. Therefore, components with a low-power requirement are better for such satellites. In the femtosatellite model by Tristancho, solar panels were attached to the cubic structure, which provides power to a 500 mA coin battery, type CR2450 [3].

Solar panels are the main source of power in most satellites. Solar panels used in previous works relating femtosatellite had solar cell efficiencies ranging from 5 % to 20 % at maximum [17]. Acquisition of low power from solar cells resulted in the development of low power consuming subsystems, i.e., the communication subsystem.

The other integral part of power subsystem is power regulation and distribution system. This part has to have a power supply board with low weight and small enough size to fit inside the structure of the femtosatellite. For the battery of the satellite, there are different options, i.e., lithium ion polymer (LIPO) batteries and the alkaline battery for small satellites. The selection between the alkaline battery and the LIPO battery is based on the weight-to-capacity ratio.

On different satellites there are different types of EPS (Electrical Power System), so for a femtosatellite either an EPS can be picked which is commercially available or it has to be designed from scratch. To save an amount of space and weight, one could design it with a voltage regulator and a voltage divider like a “P7805-S DC switching regulator” [18].

4.1 Solar Panels

Solar cells are used as the primary source of power for this satellite. The femtosatellite solar panels are selected on the basis of weight and the efficiency of the solar cell because the panels should have small weight.

One option for the femtosatellite is solar panels being used in the form of arrays. A solar array using Si cells, which are rectangular, 2 cm $\times$ 4 cm, and have a conversion efficiency of almost 12 % to 14 % . The cells have a thickness of 50 to 250 μm, but 200 μm is often used for the majority of arrays. Thin GaAs cells of about 5 μm thickness with the efficiency of 21 % have also been developed [19].

Efficient solar cells are needed in the femtosatellite, because of size limitations. There are few options: one is Triangular Advanced Solar Cells by Spectrolab which have an efficiency of 27 % $\pm$ 3 % and are triangular in shape [20]. The last one is which is the most efficient low-mass solar cell available on the market is the Concentrating Triple-Junction Solar Cell by Solaero, having an efficiency of 39 % [21].

To generate enough power to reach the mark of about 1 W to run the femtosatellite, the value of 1 W is taken from mass and power budget in table 3. To achieve this power, either the size of solar cells panels must be increased, or the efficiency of

those cells should be increased compared to efficiencies of solar cells used earlier [3] [16]. In this case, size cannot be increased because of the apparent size, and weight limitation, but the efficiency of the panels should be high enough to provide the required amount of power.

Many solar cells are developed, with efficiency up to 48 % [22]. However, few of them are available commercially, because of the high cost of manufacture. Therefore, the selection has to be limited to those most efficient solar cells which are available on the market.

In the thesis, the solar cells chosen for this project are 30 % Triple Junction GaAs Solar Cell Type: TJ Solar Cell 3G30C - Advanced (80 μm) from AZURSPACE [23]. This cell was selected because it was a highly efficient solar cell, which is readily available. This cell type is a GaInP/GaAs/Ge on a Ge substrate triple-junction solar cell (efficiency class 30 % advanced and thickness 80 μm). The end-of-life version of the 3G30C solar cell offers best EOL (end of life)-performance values and should be combined with an external bypass diode protection.

Technical Details:

- Base Material: Gallium Indium Phosphide (GaInP)/ Gallium Arsenide (GaAs)/ Germanium (Ge) on Ge substrate
- AR-coating: Titanium Oxide (TiO_x)/ Aluminium Oxide (Al_2O_3)
- Dimensions: 40 mm $\times$ 80 mm $\pm$ 0.1 mm
- Cell Area: 30.18 cm^2
- Average Weight per area: $\leq$ 50 mg/cm^2
- Thickness (without contacts): 80 μm $\pm$ 20 μm
- Contact Metallization Thickness (Silver (Ag)/ Gold (Au)): 3 μm – 10 μm
- Grid Design: Grid system with two contact pads
- Optimal Output Voltage (Vop): 2350 mV
- Min. average Optimal Output current (Iop) avg @ Vop: 505 mA
- Min. individual current Iop min @ Vop: 475 mA [23]

The solar cells are equipped with an integrated bypass diode to protect the adjacent cell in the string. All solar cells include the latest triple-junction technology, where GaInP/GaAs/Ge layers are grown on a Germanium substrate [24].

For every component discussed in this femtosatellite, both the size and weight of this solar cell are of great importance. The solar cell holds an area of 40 mm $\times$ 80 mm, which will cover the length and width of the satellite structure. In Figure 3, the area of the solar cell covering the femtosatellite can be seen.

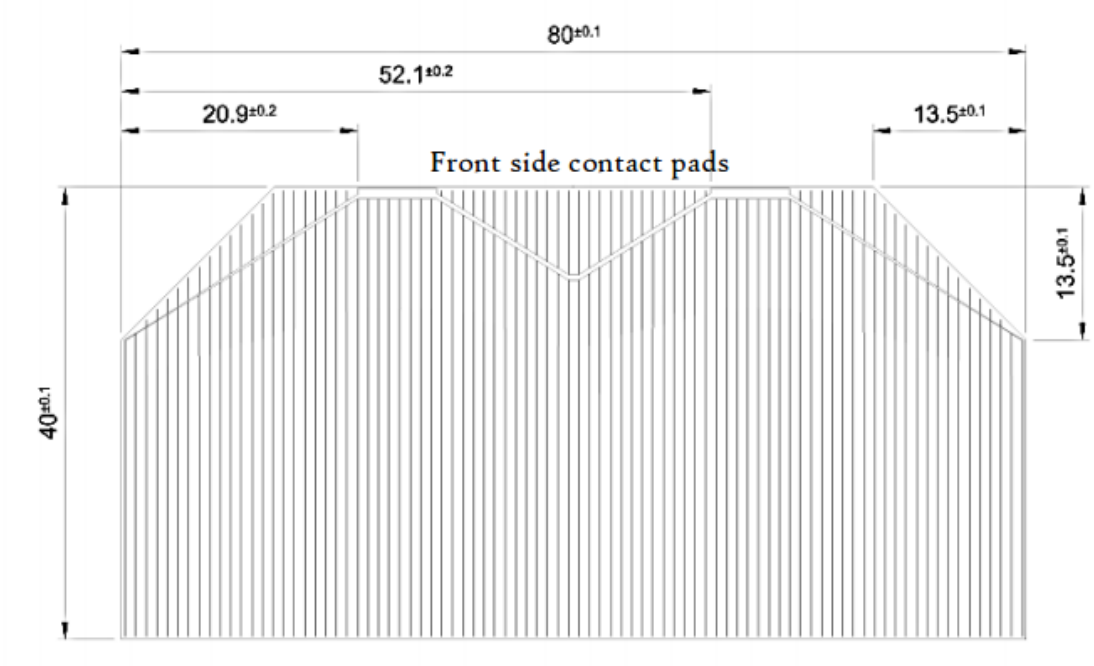

Figure 3: Solar cell dimensions and interfaces [23]

When calculating the output of the solar cell, many things should be taken into account. The area of the solar cells is of importance because if the area is increased, additional power will be acquired from them.

The output of the solar cell can be calculated by the following formula which is given as

$$E = A \times r \times H \times PR, \tag{1}$$

where E is energy, A is the total solar panel Area, r is the solar panel yield or efficiency(%), H is the annual average solar radiation on panels and PR is the performance ratio, the coefficient for losses. Shadings are not included, and tilt depends on the attitude of the satellite.

The energy output of this solar panel is calculated by taking an area of 8 cm $\times$ 4 cm, and the efficiency of 30 %. The solar constant of earth orbit value is 1367 W/m^2, 80 % of the area of the cell is exposed to sunlight, and the percentage of conversion from the solar cell is taken to be 90 %. In the case of these readings, the output power from these solar cells is almost equal to 1 Joule.

For the system, a careful analysis is performed with regarding the link budget, energy budget, and mass budget. Moreover, the operational scenarios are simulated to assure the ability of the satellite to send and receive images taken from LEO orbit.

The work also gives an overview of previous designs and studies carried out on the femtosatellite and compares them to larger satellites in terms of cost, structure, and also functionality.

4.2 Charge Controller

The charge controller is a necessary part of the power subsystem, and it distributes and regulates power. The charge controller takes power from the battery and the solar panels. It supplies power to the microcontroller, which transfers power to all the components. This charge controller takes power from the solar panels and provides it to the battery for charging. This battery then provides power to the system in the case when direct power is not enough. The power draining from the battery and its charging can both occur at the same time.

A component called Sunny Buddy Solar Charger V13 was selected to serve as the solar charge controller [25]. Sunny buddy is a small maximum power point tracking(MPPT) solar charger for single-cell LiPo batteries. [25].This MPPT solar charges takes out the maximum output power from the solar cell and provides it to the load. It's setup is easy you just have to connect solar panel at one point and batteries and load at the other point.

- Input supply voltage regulation loop for peak power tracking in (MPPT) solar applications
- It has programmable charge rate up to 2A
- It has wide Input Voltage Range: 4.95V to 32V
- Japanese solderless terminal (JST) 2.0 connector
- Termination is user selectable: C/10 or on-board termination timer
- No V_{in} blocking diode required for battery voltages $\leq$ 4.2V
- Charge LIPO battery through solar power or USB
- Resistor programmable float voltage up to 14.4V accommodates Li-Ion/Polymer

Specifications:

- Fixed frequency of 1MHz
- Open-Collector binary-coded status pins
- 2.5% C/10 detection accuracy
- 5% charge current accuracy[25]

The small size of sunny buddy charge controller make it suitable for a femtosatellite compared to other charge controller systems which have a slightly larger size than this, like the charge controller subsystem for Aalto-2 [26].

The size of this charge controller board is also smaller than the size of the PCB board for the microcontroller, which makes it easier to mount on a microcontroller. Furthermore, the smaller size of charge controller helped to achieve the lower weight limit dedicated to the femtosatellite. The sunny buddy is shown in Figure 4.

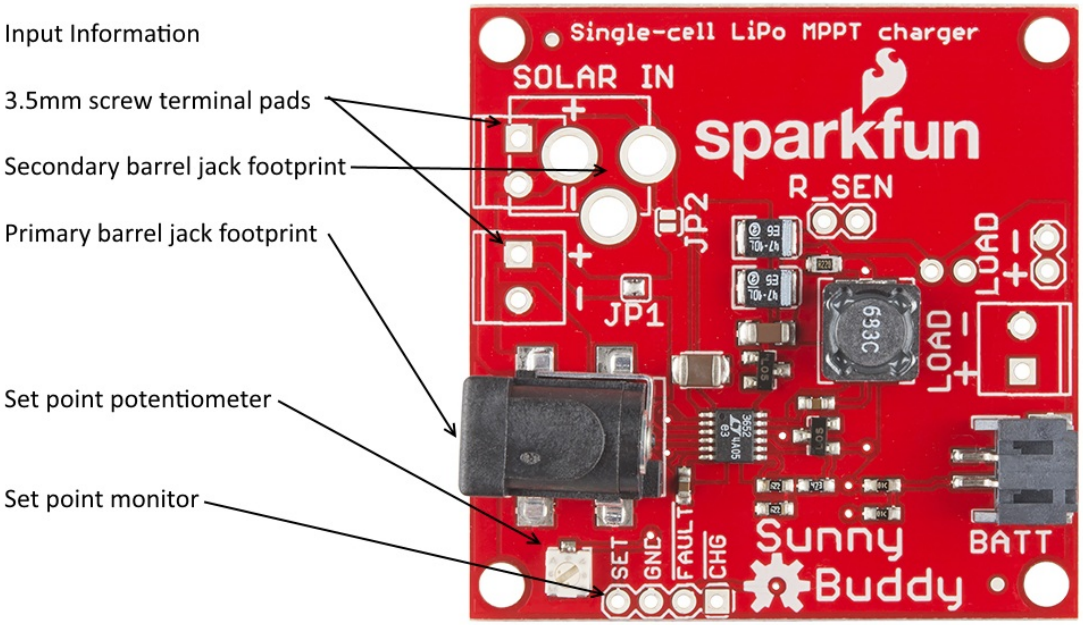

Figure 4: Details of the input for the sunny buddy charge controller[25].

Figure 4 depicts the input information for the charge controller board. On the left side, apart from the 3.5 mm screw terminal pads, it has one barrel jack connection for the power from the solar cell. It has one secondary point for the barrel jack connection as well. If two solar cells are used then solder jumper one JP1 has to be cleared but solder jumper 2 JP2 has to be closed, they can be seen in figure 4.

On the right part of the sunny buddy are the output connections to the battery and the load which in this case is the raspberry pi zero. It also has fault indicator and charge indicator as well. It comes set to a maximum charge current of 450 mA.but he auxiliary sense resistor footprint allows it to have around 550 mA but the resistor ca be desoldered if less than 450 mA is desired.

The raspberry pi zero can be connected to either the 0.1 in or 3.5 mm spaced pads on the right side of the board. The charge control will be done by raspberry pi zero, whether to use direct power from solar cell or take power from the battery.

The output information of sunny buddy is presented in Figure 5 which explains the working operation of the device. In figure 5 the output information of the charge controller is highlighted, showing that it can provide power to both the lithium battery or the solar panel. Both the output ports are connected in parallel.

4.3 Battery

The battery within the satellite is the part of the power subsystem, which stores power from the solar cells or any other power source. In the case of femtosatellite, the battery should be light enough to be suitable for such a small satellite, but on the other side, it should also have enough storage or capacity to ensure that satellite

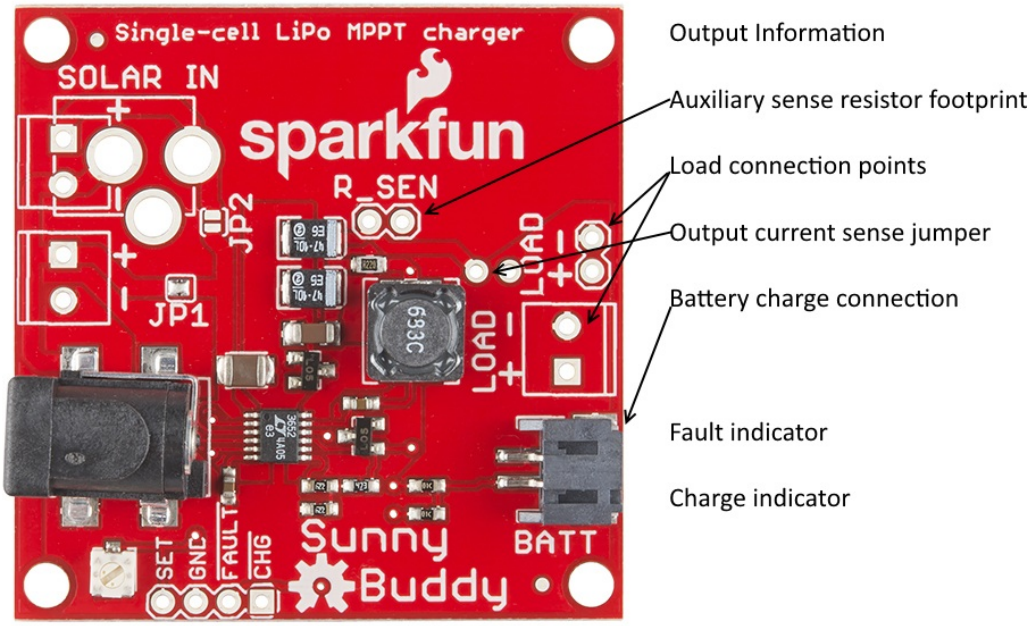

Figure 5: The connection of all the parts of the device [25].

should not run out of power.

Therefore, the qualities on which the battery should be selected are: first, that the battery should be suitable in terms of weight for this type of satellite; second, that the battery should have enough power storage capacity to match the needs of the computing and communication subsystems of this femtosatellite; and, third, is that it should work in a vacuum.

The battery chosen for this femtosatellite was the Lithium Ion Polymer Battery - 3.7 V 1200 mAh from Adafruit [27]. This battery was chosen for its lightweight properties and storage capacity of 1200 mAH. Lithium-ion polymer (also known as 'lipo' or 'lipoly') batteries are slim, lightweight and powerful. The output ranges from 4.2 V when fully charged to 3.7 V. This battery has a capacity for a total of about 4.5 Wh. In Figure 6 there is a picture of the battery.
The batteries come pre-attached with a 2-pin JST-PH(PH is the type of JST connector) connector and include the necessary protection circuitry. The included protection circuitry keeps the battery voltage from going too high (over-charging) or low (over-use) which means that the battery will cut-out when completely flat at 3.0 V. It will also safeguard it against output shorts [27].

The features of the LIPO battery are:

- Storage Humidity: 65 ± 20% RH (Relative Humidity).
- Overcharge Threshold: 3.95 V
- Over discharge Threshold: 2.3 V

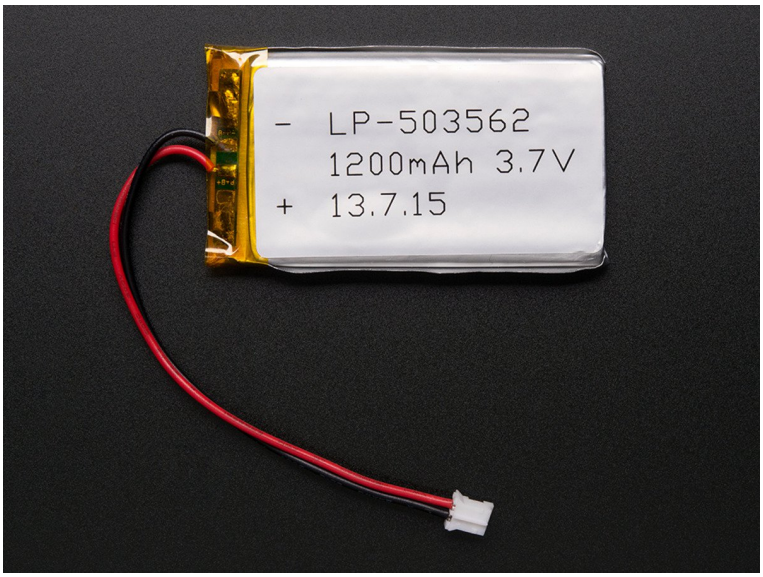

Figure 6: The image of the battery with the 2-pin JST-PH connector [27].

- Weight: 23 g
- Dimensions: 34 mm × 62 mm × 5 mm
- Capacity: 1200 mAh
- Nominal Voltage: 3.75 V
- Working temperature: 0° - 40° C (safety from peak temperature will be provided by kevlar shielding)
- Storage temperature: - 10° - 45° C.
- Charge Cut off Voltage: 4.2 V
- Standard Charge Current: 0.2 C_5A (C_5 means five hour discharge time, A means Ampere)
- Standard Discharge Current: 0.5 C_5A
- Impedance: $\leq 50\ \Omega$
- Cell Voltage: 3.7 - 3.9 V

Power is provided to the charge controller through the solar cell, but in case power from the solar cell is not enough, or the satellite is in eclipse, power from the battery is used. This battery can provide the power of 4.5 W for an hour. The maximum time for the communication is about 2 minutes due to the limited beamwidth of directive circular patch antenna required for connection with the ground station. The transmitting power for this communication is 1.5 W according to the PA and transmitter rating. 0.5 W is used for different tasks constantly, i.e., power is

provided to the microcontroller and other components. So the total power used during transmission is almost 2 W, the battery can easily provide this much amount of power.

5 Antenna Subsystem

An antenna is a transducer that converts radio frequency (RF) fields into alternating current or vice versa. The antenna is the wireless connection of satellite with Earth. Earlier works on small satellites like Aalto-1 and Aalto-2 include one or more antennas, one for communication and others for location information through GPS(Global Positioning System) and other functions [28]. The main antennas in the satellites mentioned were working at the UHF (Ultra High Frequency) band.

The S-band antenna from Aalto-1 uses 2.4 GHz frequency for communication purposes. S-band antennas in Aalto-1 were directive while UHF band antennas are Omni-directional. S-band antennas are usually smaller, and UHF antennas are larger, the reason being that the wavelength of S-band antennas is smaller than UHF antennas. This reason makes them suitable for a femtosatellite.

Different antennas are recommended for the femtosatellite such as the dipole array, the patch antenna, the slot antenna and the synthetic aperture antenna [29]. Some other options for this kind of satellite are a micro strip patch antenna [30], a printed dipole antenna array [31], a Zero Index Metamaterial (ZIM) [32] patch antenna and a slot antenna [33]. One other mentionable type is a 61.4 mm square patch antenna, having a gain of 12 dBi at 2.45 GHz which is suitable for small satellites [34].

Analyzing by mass and size, one possible antenna is a ceramic antenna array, in which each ceramic antenna acts like a dipole and the collective gain for the whole array is about 6 dB which can be seen in Figure 7.

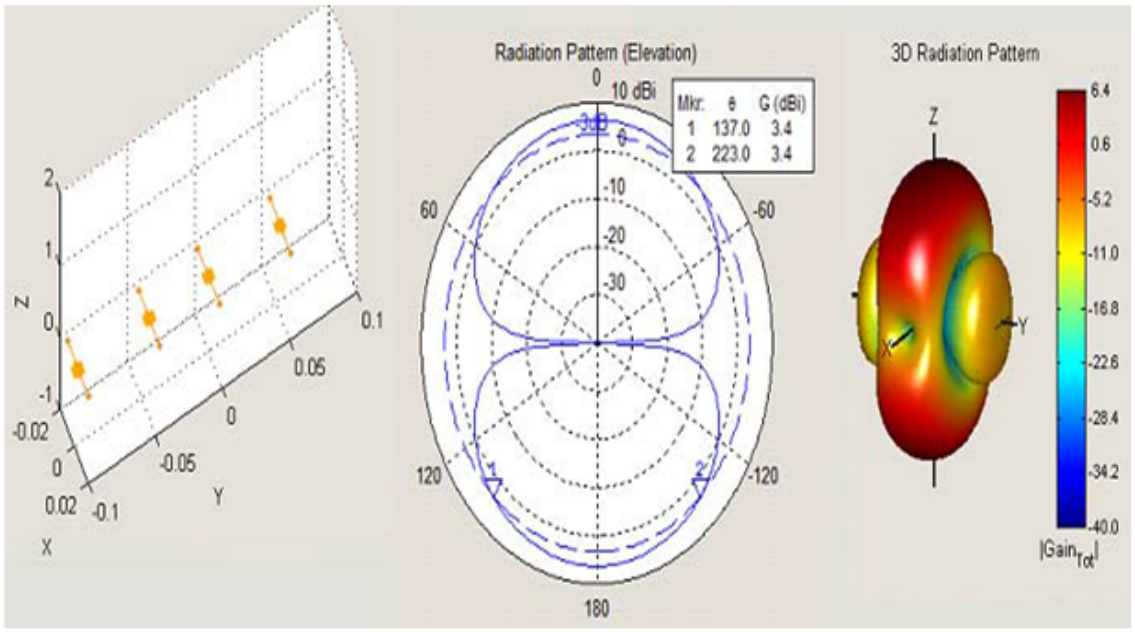

Figure 7: The ceramic antenna array, their arrangement, radiation pattern (elevation) and 3D radiation pattern [35].

From the above examples for a femtosatellite, an antenna can be carefully selected

or made, having same qualities. The antenna would be directional due to low power requirement. Another reason for selection of directive antennas is that they have higher gain than omnidirectional antennas.

To match, the requirements, a circular patch antenna with an air gap was selected, based on the compromise between high gain and broader beamwidth region. A patch antenna was chosen over others, mainly because of its smaller size and because it is lightweight in comparison to other antenna types while providing a high gain at the same time. Finally, an air gap was included in the antenna to increase further the gain while keeping the same small size.

The antenna of a femtosatellite has requirements of high gain, small weight, in terms of tens of grams, and broader beamwidth in order to have more extended connection range with the ground station. Therefore, a circular patch antenna with an air gap was selected for the femtosatellite.

5.1 Background of Circular Patch Antenna

A patch antenna is usually in the shape of rectangular sheet or patch mounted over a ground plane which is a larger sheet of metal. The patch antennas are beneficial in the sense that they have low mass, they can adjust to any geometrical shape, they have easy integration with different structures and lower fabrication cost. Their main disadvantage is that they have small bandwidth [36].

Within different types of a patch antenna, the most common are the rectangular and circular patch. Following the rectangular patch, the circular patch is probably the most common shape. It can be made slightly smaller than its rectangular counterpart, but with a small loss in gain and bandwidth.

The circular patch has some favorable properties, but its high directivity was the reason why it was selected in this work, as shown in Figure 8. It also has received much attention not only as a single element but also in arrays.

The surface waves in patch antennas are "modes" of propagation supported by the ground substrate. Surface waves propagate in a cylindrical fashion around the excitation port. The electromagnetic waves are reflected back through the ground plane substrate. The surface waves propagate until arriving at the edge boundaries, after which they are diffracted and reflected by the edges [38].

Different modes are supported by the circular patch antenna; this is done by treating the ground plane, patch, and the material between the two as a circular cavity. Compared to the rectangular patch, the modes that are supported mainly by the circular microstrip antenna are those whose substrate height is small ($h << \lambda$), i.e., TM^z. TM is the Transverse magnetic mode, lambda is wavelength, where h is the height of thickness of the substrate, z is the direction in which the wave is propagating, and z is taken perpendicular to the patch [37].

There are two degrees of freedom to control which are length and width for the dimensions of the patch for the rectangular microstrip antenna. Therefore, by changing the relative dimensions of the width and length which is width to length ratio, the order of the modes of the patch can be changed [37].

Nonetheless, the radius of the patch is the only one degree of freedom which can

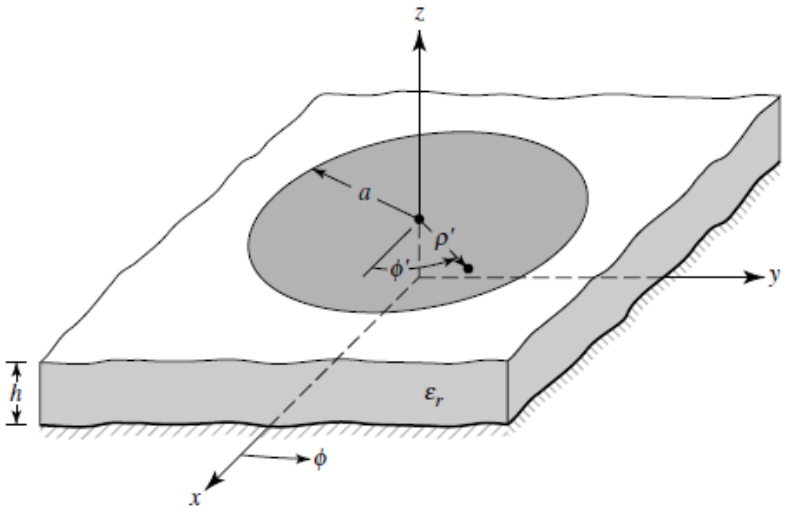

Figure 8: The main components of the Circular Patch antenna [37].

be controlled in the circular patch. This freedom not only changes the absolute value of the resonant frequency of each mode but it also varies the order of the modes.

Apart from using full-wave analysis, there is only one trick of applying the cavity model by which the circular patch antenna can be analyzed in a better way. Two perfect electric conductors make up the cavity, one is at the top and the other at the bottom to represent the patch and the ground plane of the antenna. This patch also includes a cylindrical perfect magnetic conductor around the circular periphery of the cavity. The dielectric material of the substrate is allowed to be reduced beyond the extent of the patch [37].

Modeling the circular microstrip patch antenna (Figure 8) as a cylindrical cavity, bounded at its top and bottom by electric walls and on its sides by a magnetic wall, which can be resonant height-independent TM modes, the electric field inside the cavity can be written as

$$E_z = E_0 J_n(kp) cos(\phi)', \tag{2}$$

where $J_n(kp)$ is the Bessel function of order n, $k = (\omega/c)\sqrt{\epsilon_r}$, ($\omega$ is circular frequency, c is the velocity of light in free space, ϵ_r is the relative dielectric constant of the substrate) and (p, ϕ', z) are the cylindrical coordinates. The characteristic equation for the resonant frequency of a circular microstrip patch is given by

$$J_n'(ka) = 0, \tag{3}$$

where a represents the radius of the circular patch. For the dominant mode (TM11), the resonant frequency can be obtained using the equation

$$f_r = \frac{1.8411c}{2\pi a_e \sqrt{\epsilon_r}}, \tag{4}$$

where a_e is the effective radius of the circular patch and is given by

$$a_e = a[1 + \frac{2h}{\pi a \epsilon_r}(\ln \frac{\pi a}{2h} + 1.7726)]^{1/2}. \tag{5}$$

where h is the height of the substrate [39].

5.2 Design and Simulation of Circular Patch Antenna with Air Gap in CST

The CST software was used for the design and simulation of the antenna because this software provides a user-friendly environment, which works with a wide range of frequencies. The dielectric material selected for this antenna of the femtosatellite is Rogers RT6010 (lossy) which is present in the CST library. This material possesses properties such as high dielectric constant for circuit size reduction, tight ϵ_r and thickness control for repeatable circuit performance, space-saving circuitry, suitability for patch antennas, which is best for satellite communications systems.

The work on antenna started when the dielectric slab was made in CST. It was created by selecting the brick tab from the modeling window in the CST. The length and width of the antenna is 4.6 cm × 4.6 cm, and the thickness is 3 mm.

The length, width, and thickness are kept to the minimum because the mass of the antenna board is kept to its lowest limit, while the gain is maintained and beamwidth of the antenna is increased to the maximum possible limits in that size.

Just below the dielectric slab, there is the ground plane, which gives better directivity. It is made using the same procedure as the dielectric slab, and it also possesses the same parameters like the dielectric slab, except the thickness of the ground plane is 0.3 mm.

After the ground plane, an air gap was introduced. The basic idea for adding the air gap, which in this work is a vacuum gap in between two dielectric slabs, was to further increase the gain, without the size of the antenna being increased. The gap between the dielectric slabs also determines the matching of the antenna and the gain of the antenna. So the vacuum was selected according to the requirements of the antenna, but this type of gap can induce a different kind of changes in antenna characteristics for different kinds of patch antennas. Figure 9 shows the side view of the antenna in which the air gap within the dielectric slab and the ground plane is visible.

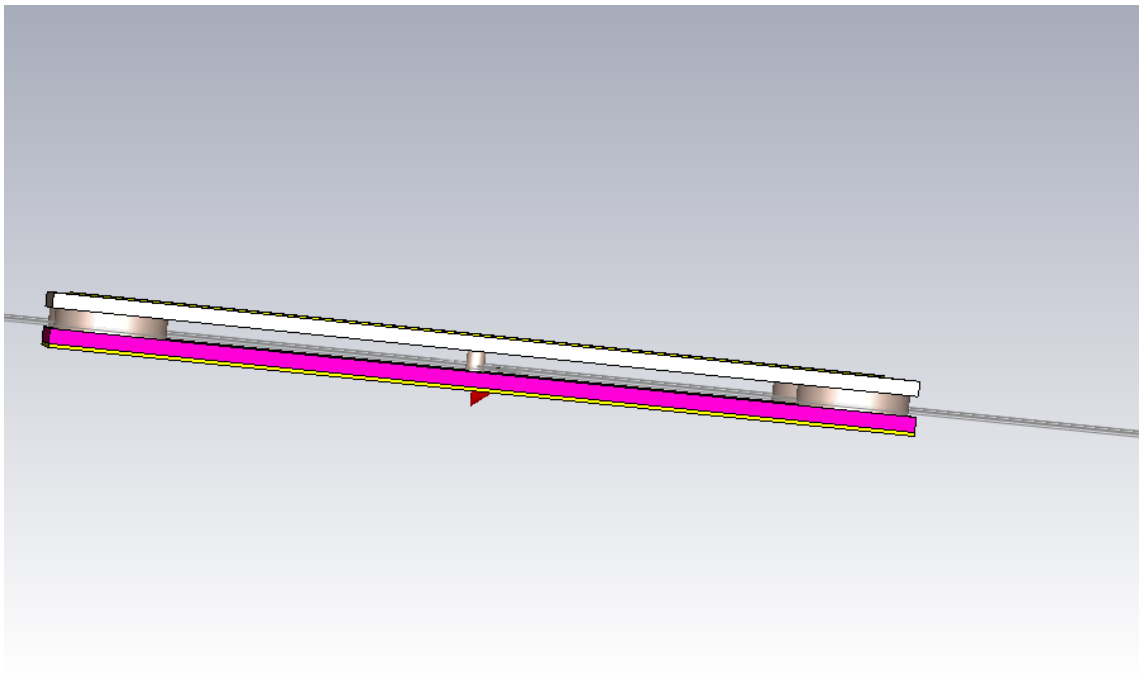

Figure 9: Side view of the antenna, two dielectric planes, ground plane (red) and the four connecting parts between the two dielectric slabs are indicated.

After the air gap is introduced, a dielectric slab is placed in the upward direction, upon which the patch is planted. This is also visible in Figure 9. The dielectric slab has the same thickness, length, and width of the bottom dielectric slab mentioned earlier. In the figure, they are presented in two different colors to show the difference

between the upper and lower slab.

In between the two dielectric slabs, there are four connecting cylinders, to support the full antenna structure with the vacuum gap. The radius of the cylinders is 0.5 mm, and the length of the cylinders is 1 mm. The radius of the cylinders has a substantial effect on the matching of the antenna as well as on the weight of the antenna. Therefore, it has to be made in a way to make it suitable for the femtosatellite.

About the upper dielectric slab, the trace of the circular patch is placed. The material of the circular patch is copper with the thickness of 0.1 mm. The radius of the circular patch is one of the necessary points in the design of the antenna as it deals with the matching of the antenna. The radius of the circular patch is 21 mm. In Figure 10 top view of the circular patch is displayed. In this Figure, a rectangular

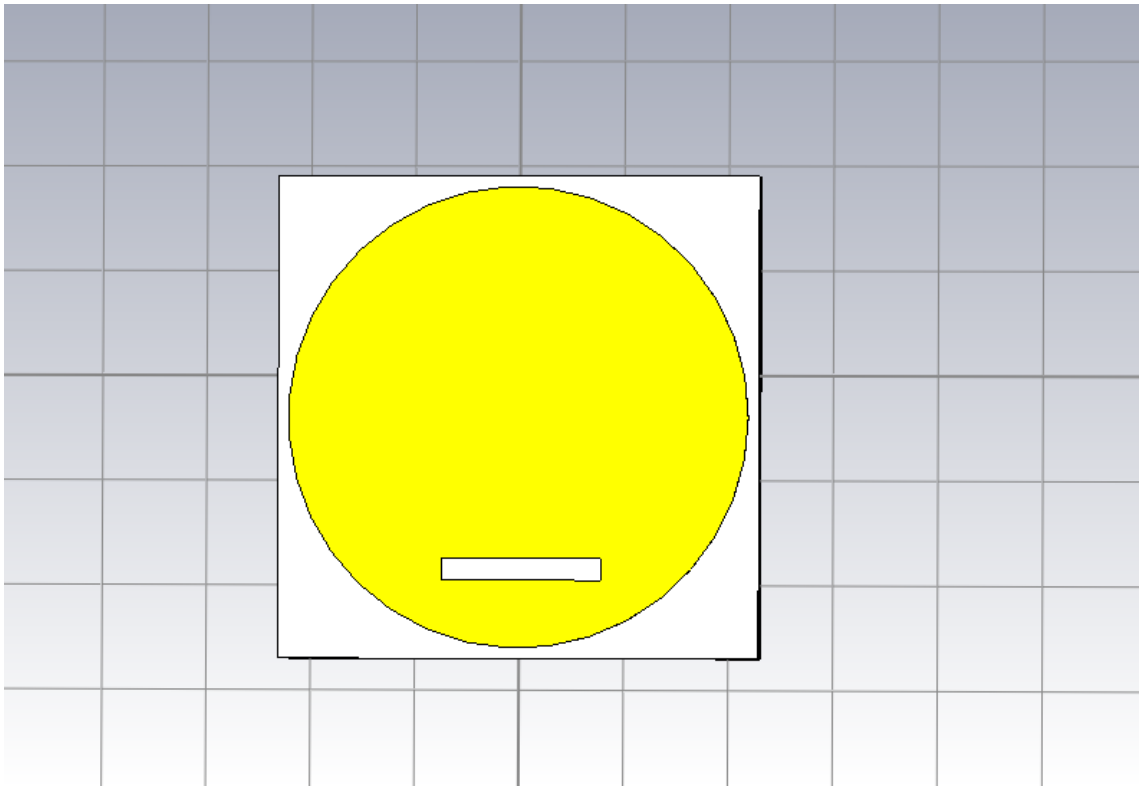

Figure 10: Top view of the circular patch antenna with a rectangular gap inside the circular patch.

gap in the circular patch is present. It was placed in a rectangular patch to match the specific frequency of the S-band. The thickness or height of the gap is the same as the thickness of the circular patch.

The length and width of the circular patch are 15.022 and 2.06 mm respectively. Increasing or decreasing those parameters shifts the frequency under consideration to a different point on the frequency band. The position of the gap in the patch is also a point of focus, as not all positions in that patch correspond to the same frequency band. Therefore, the position for the gap chosen in the patch of the antenna was

slightly below the point where the feed touches the antenna if it is viewed from the top view. This point responds to the 2.4 GHz frequency point.

This gap was made in the patch when a rectangular brick was introduced; the brick has the length, width, and thickness of the gap and it comprises a different material than the material of the patch. Therefore, the coordinates are given to the point where the gap is needed. There are multiple options in software, and one of this option is to cut the shape, which then creates the gap.

The next step in the design and simulation of the circular patch antenna, which is also evident in Figure 9, is the port design of the antenna. The port consists of many parts, and its sole function is to provide the power supply to the circular patch. The different parts of the port include one cylindrical pin and two coverings on the pin at two different points around the pin. Figure 11 shows the side view of the port in which different parts are indicated.

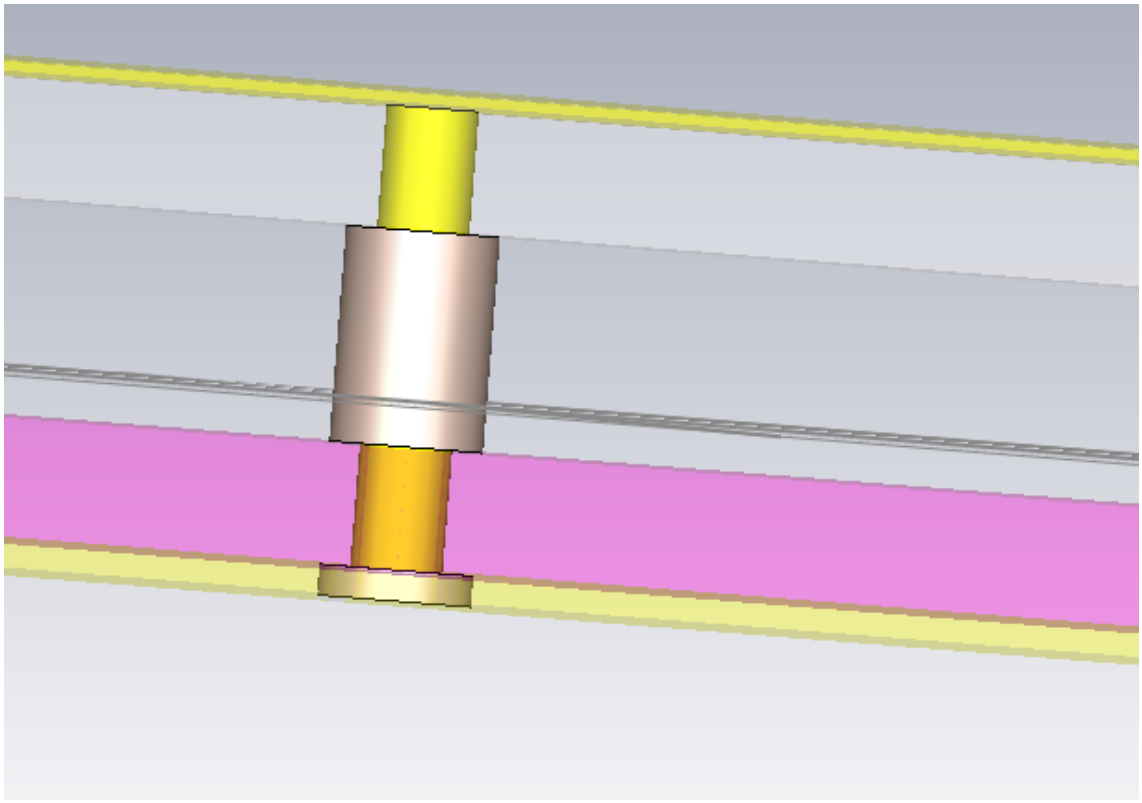

Figure 11: Three parts of the antenna port: the cylindrical pin, lower small covering, and long upper covering for the air gap.

It is evident from Figure 11 that the cylindrical pin started from the ground plane going through the dielectric material, then it goes through the air gap and then again through the dielectric to finally reach the circular patch antenna. The radius of the pin is 0.2 mm, and the length of the pin is 20 mm. The pin was made through the cylinder tab in modeling window.

The lower covering is in place in order to restrain the pin from shorting with

the ground plane of the antenna. It is constructed with a torus shape inside the modeling tab, which is a cylinder but it is hollow from the inside. The inner radius of the lower cover is the radius of the pin, 0.2 mm and the outer radius of the covering is 0.5 mm. Therefore, the thickness of the covering is 0.3 mm. The length of the covering is the same as the thickness of the ground plane 0.3 mm.

After the ground plane, the pin goes inside the lower dielectric slab then into the air gap where it needs covering again. The inner and outer radius of the covering is the same as the lower covering. The length of the coverage varies from the dielectric substrate, because of the difference in thickness of the air gap and ground plane. Therefore, the length of this covering is 14 mm. This length is due to the need to avoid any interference from the air gap.

After the air gap, the pin goes through the dielectric slab to finally reach its destination at the circular patch, which is above the dielectric slab. Before the pin is placed in the antenna structure, holes were made with the radius of the pin to avoid materials being mixed. In the ground plane, an extra hole was made for the covering too.

For the supply of the port, the discrete port is selected. The discrete port starts from the edge of the pin in the ground plane going through the covering to reach the ground plane, which is depicted in Figure 12.

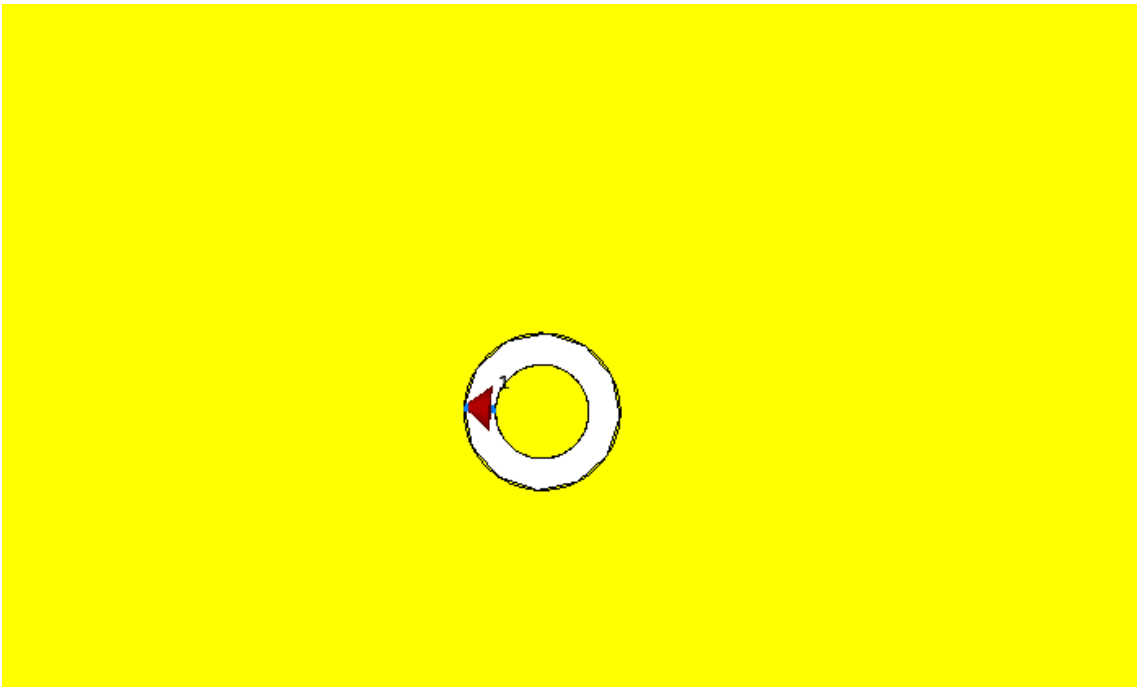

Figure 12: Bottom view of the port, the port inside the ground plane is shown.

The position of the port is again the crucial point because it plays a role in the matching of the circular patch antenna. With the design of the port, the design of antenna is completed.

5.3 Radiation Pattern of the Circular Patch Antenna

In the field of antenna design, the term radiation pattern (or antenna pattern or far-field pattern) refers to the directional (angular) dependence of the strength of the radio waves from the antenna or other source [40]. The radiation pattern is one of the significant results for this antenna in CST. There are two main reasons behind this: one is that the gain of the antenna is critical and the second is that the radiation pattern shows half-power beamwidth. The 6 dB target was taken from the link budget discussed later in the thesis, to have enough gain for the communication link. Therefore, the work started when the goal of achieving more than 6 dB of gain with the smallest size possible was made. In Figure 13, the gain of the circular patch antenna with an air gap is illustrated.

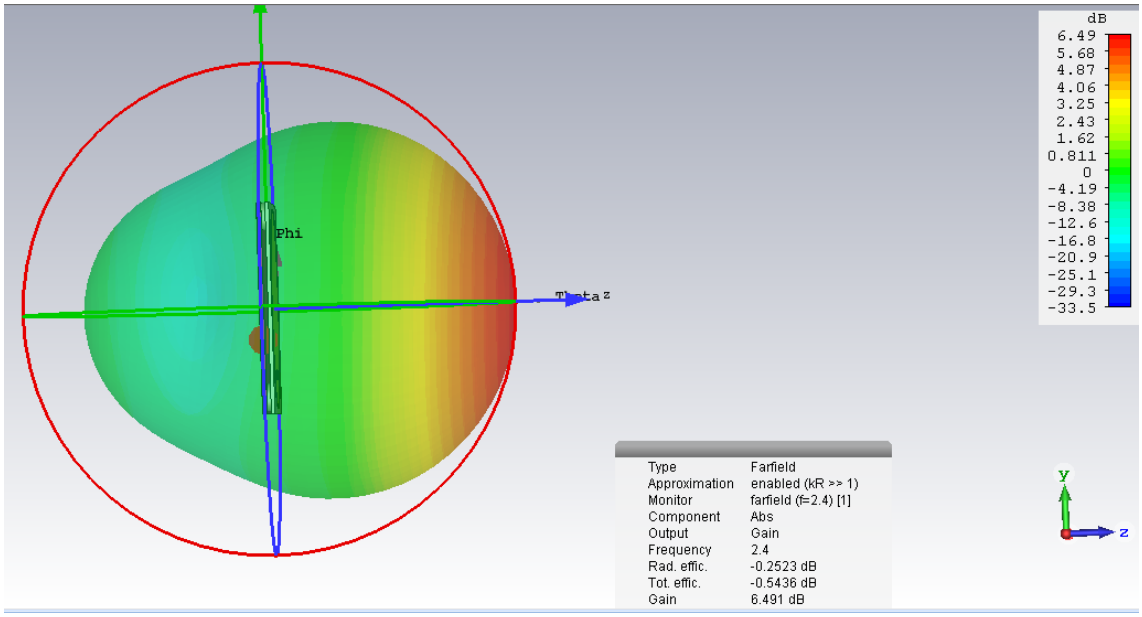

Figure 13: Antenna power gain in dBs which is indicated in the bar in the left corner of the figure.

This Figure 13 also gives the values radiation and total efficiency besides the total gain of the antenna, which is 6.66 dB in the figure.

The values of radiation efficiency and total efficiency are equally important, which are -0.1521 dB and -0.9475 dB respectively, as they are indicative of the sum that makes up the gain. These values account for the losses in radiation and losses in the antenna.

One other primary value not shown in Figure 13 is directivity: its value is 6.82 dB, which has the same kind of pattern except a slightly more power. The direction of the radiation pattern is also given in Figure 14, which shows how the radiation is directed in the forward direction and that the antenna is directional. Another part, which was essential to check in the radiation pattern, was the half-power beamwidth, which is indicated in the polar diagram of the radiation pattern. It is essential in the case of a femtosatellite because the beamwidth of the antenna determines the

distance of coverage of antenna, as our satellite antenna is going to cover concerning connectivity with the ground station antenna.

The beamwidth of the antenna is visible in the polar plot of the radiation pattern. There are two polar plots of the radiation pattern, the first is constant phi and the second is the constant theta pattern. The beamwidth of the antenna is present in the constant theta polar plot. The constant phi polar plot in represented in Figure 14.

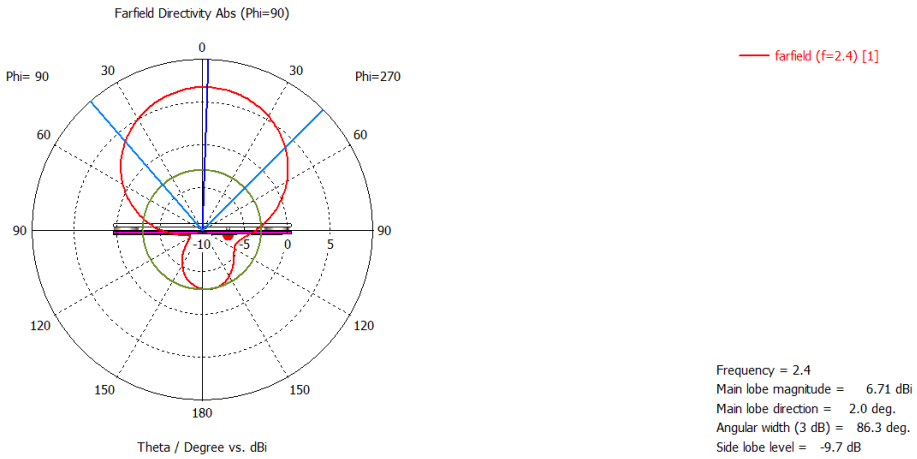

Figure 14: Side view of the circular patch antenna along with the constant phi plot of the radiation pattern

In the constant phi polar plot, the beamwidth of the circular patch antenna with an air gap is 86 degrees. If the speed of the satellite in orbit is known, then, with the help of the beamwidth, the distance of connectivity is calculated.

The gain and beam width of the antenna is mostly controlled when the thickness of the dielectric constant and the air gap between the dielectric slab is controlled. The main lobe magnitude of the constant phi polar plot is 6.71 dB which is evident in Figure 14 and its direction is 2.0 degrees. One extra factor, which is shown in the figure of the constant phi polar plot is the side lobe magnitude of -9.7 dB. The sidelobe magnitude of the constant phi is vital as it points to the losses in the radiation pattern in the unintended direction.

The next part of the radiation pattern polar plot is the constant theta polar plot, which represents the top view of the radiation pattern. This polar plot is also shown in Figure 15. The constant theta pattern indicates the main lobe magnitude of 3 dB in the top view of the radiation pattern and its direction of the 309 degrees.

Other salient factors of the radiation pattern are shown such as the axial ratio which tells about the polarization type of the radiation. The value of the axial ratio of the radiation pattern is 40 dB which confirms that the polarization of the circular patch antenna with the air gap is not circular polarization as the represented in Figure 16.

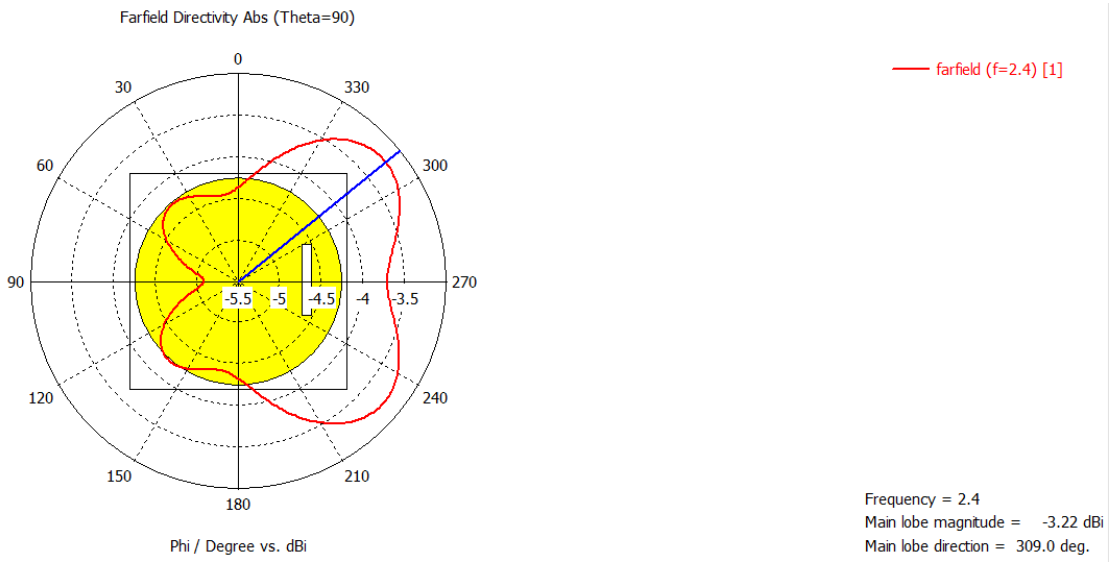

Figure 15: Top view of the circular patch antenna indicating the constant theta polar plot.

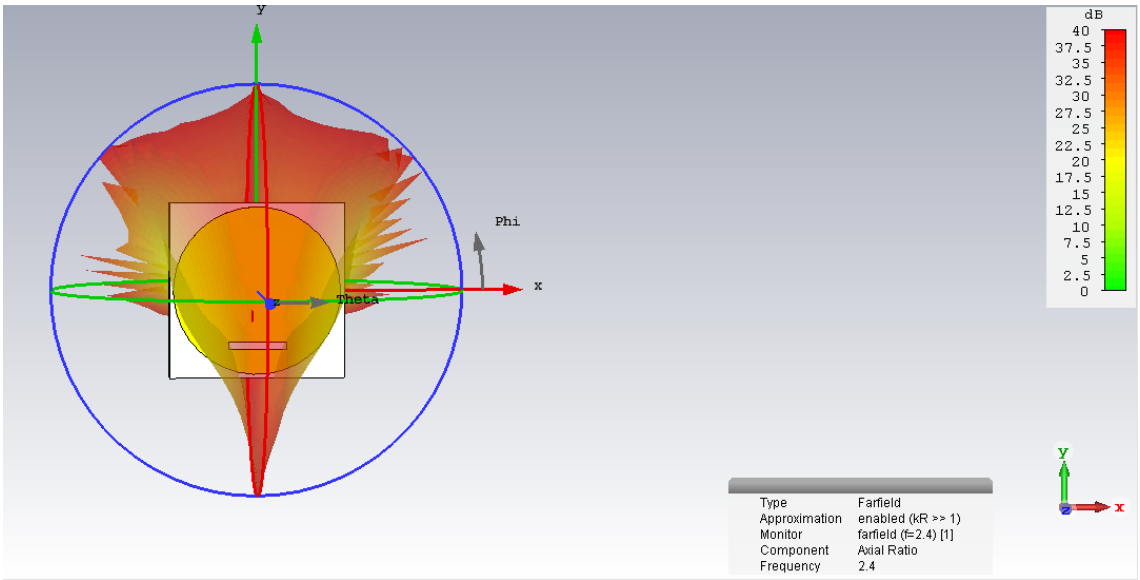

Figure 16: Radiation pattern the axial ratio in the power of dB.

5.4 Return Loss or S11 Parameter

The S11 parameter or the return loss is another crucial result of the design of the circular patch antenna design in CST. It represents the amount of power transfer to the antenna and losses inside the antenna at the specific frequency of interest.

The chosen frequency band for the circular patch antenna with the air gap is the S-band at the point of 2.4 GHz. However, the matching at the frequency of 2.4 GHz at a small antenna of the circular patch was difficult to attain because the smaller the antenna, the higher the frequency. Therefore, many adjustments to the antenna

designs were made to reach the required frequency matching point.

The adjustment to the antenna design included changing the port position in the ground plane. A rectangular gap in the circular patch trace and also the thickness of the air gap affects the return loss. The S11 is shown in Figure 17.

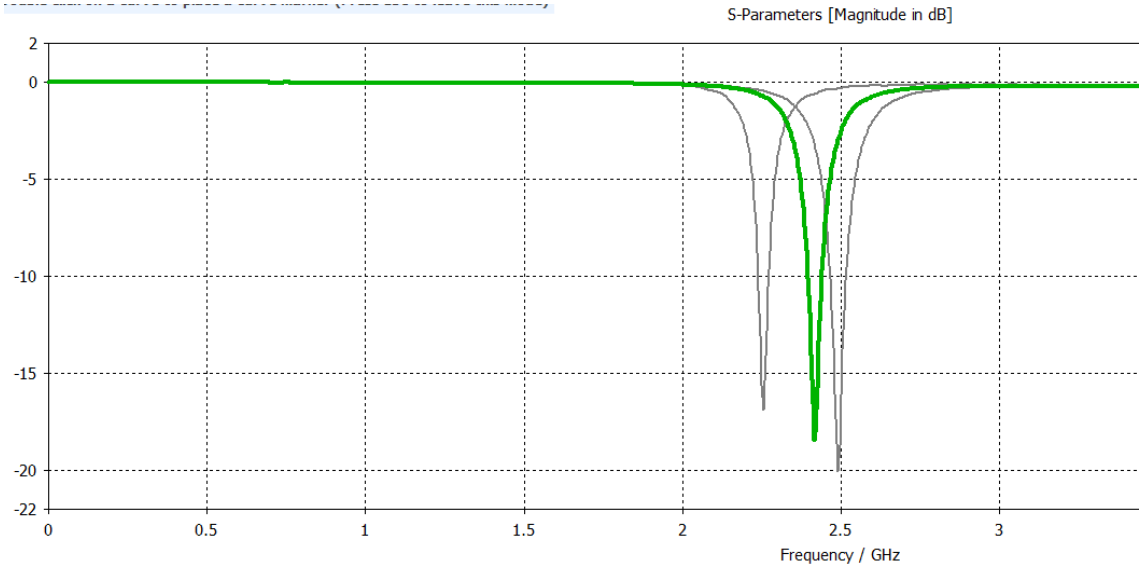

Figure 17: The figure represent the reflection at the point of 2.4 GHz, which is -18 dB.

The level of -18 dB reflection level and it indicates the power loss. This value of -18 dB presents the slight amount of power is lost during the radiation process. The bandwidth of matching under -10 dB is about 50 MHz. The two grey lines show the return loss of different thickness levels of the air gap.

6 Communication Subsystem

Communication is a significant part of this femtosatellite design. It is the link to the satellite, through which information is sent and received. This subsystem communicates with the ground station, receiving and transmitting information from the ground station.

An obvious challenge for such a small satellite is the communication link between the ground station and the satellite. It is not unreasonable to deduce that the uplink is not as much difficult to implement as the downlink because transmit power from the ground station can be increased to cover any shortfalls in the communication for the uplink to the satellite. However, the satellite position must be known to avoid pointing losses with the high gain antennas, that must be used [41].

A communication subsystem contains an antenna, a transceiver, a power amplifier (PA), a low noise amplifier (LNA), switches for selection between PA and LNA selection and matching circuitry around them. Much of hardware and equipment used for radio can be used independently and do not need specialized equipment. Therefore, the operations done by the transceiver like encryption, modulation, and demodulation is operated by single piece of hardware, meaning there is no need to change them. However, in some cases, add-on modules help in order to change to different frequencies [42].

The frequency selected for the communication was the S-band frequency, and it is used for different reasons. One of these reasons is the GeneSat-1, and Can-X2 missions, which used the S-band frequencies for data transmission. The data throughput of Can-X2 was more than twenty-two CubeSat missions had achieved in a total of five years, in which UHF frequencies were used. This point highlights the fact that higher frequencies should be used when more data throughput for the satellite is required. Furthermore, since rf transmit power used by Can-X2 was 500 mW, the use of S-band communication systems is suitable for the CubeSat power constraints [43].

6.1 Link Budget of the Satellite

The link budget is the essential part of calculations for satellite communication before it is sent to orbit. It reveals the feasibility of the communication link between the satellite antenna and the ground station.

At the ground station, a 3 m paraboloid reflector is used at the S-band. It has the gain of 41.34 dB. The transmitter antenna gain is more than 6 dB, but a 6 dB marginal value was taken in table 2 to complete the required limit to communicate with the satellite. In this table 2, the signal to noise ratio of the link budget is about 17 dB, which is sufficient for sending high-quality images to Earth. Different types of losses were also considered in the link budget including path and polarization loss.

There is one constant value which is the Boltzmann Constant (K). There are many variables in this link budget which are: Transmitting Power (Pt), Gain of Transmitting Antenna (Gt), Distance (R), Distance of Horizon (d), Height (h), Gain of Receiver (Gr), Noise Power (Pn), Receiver Power (Pr) and Effective or Equivalent

Isotropic Radiated Power (EIRP).

Link budget calculations started when the receiver antenna gain was calculated. This receiver antenna is located at Aalto University premises at the time when the thesis was being written. The gain was calculated according to the S-band frequency of 2.4 GHz. This gain is calculated by the diameter of the antenna, its efficiency, and the frequency used.

The distance for the orbit was selected as 400 km, and the distance from the horizon was taken as 2292 km with the formula mentioned in Table 2. This horizon distance calculation is in the case of the paraboloid antenna when it can move about its axis, but in this case, it is fixed at one location. Therefore, to avoid any miscalculations, the values in this table are taken from the horizon.

The values of different variables such polarization mismatch, misalignment losses and pointing losses in the table are taken from various sources. Those source include different books and articles which are related to the base station values of Aalto-1 and Aalto-2 satellite from their respective link budgets [44] [43] [28].

The beamwidth of the antenna is about 86 degrees, and the height of the orbit is 400 km for this femtosatellite. With these parameters, the distance in which the femtosatellite comes in contact with the base station can be calculated. When half angle of beamwidth is taken, which it is 43 degrees and the height of the satellite, the distance calculated when a triangle of about 750 km through simple tangential angle calculation is taken, is illustrated in Figure 18.

The speed of the satellite in the orbit can be calculated with the given formula

$$v = \sqrt{\frac{Gm_E}{r}}. \tag{6}$$

According to the equation, the calculated speed in the 400 km orbit is 7.7 km/s, where G is the gravitational constant, v is the velocity of the satellite, m_E is the mass of Earth and r is the radius of Earth. With this speed, a distance of 750 km is covered in 93.75 seconds or 1.5625 minutes.

6.2 Communication System Design

For the communication system, a particular communication chip of (nRF24L01) was selected. This is a single chip 2.4 GHz transceiver. It has low power and high-performance capabilities. Fewer amounts of components are required for this chip to create fully functional radio system.

The nRF24L01 is configured and operated through a Serial Peripheral Interface (SPI) connector. With the help of this interface, the register map can be used. Register map is the place where information about different registers is stored, i.e., configuration of registers. The register map is accessible in all operation modes of the chip and contains all configuration registers in the nRF24L01.

The embedded baseband protocol engine (Enhanced ShockBurst^{TM}) supports from different modes of manual operation to advanced autonomous protocol operation and is based on packet communication. Internal FIFO's(First In First Out) ensure a smooth data flow between the radio front-end and the system's Microcontroller Unit

Table 2: Proposed link budget of satellite

Link budget for Femto Satellite	Decibels						
Transmitting antenna Pt	0						
Gain of Transmitting antenna Gt	6						
EIRP		6 dB					
Distance R		400 km					
Distance from Horizon		2292 km		formula d= √Rh+h²			
Frequency f		2.4 GHz					
Aperture receiving antenna		3 m					
Efficiency for receiving antenna		60 %					
Polarization loss	-3						
Path Loss	-167						
Gain of the receiver Gr	41						
Mismatch losses at receiver	-3						
Missalignment losses	-1						
Atmospheric losses	-1	Including rain, ionospheric and other losses					
Pointing loss	-1						
Space Craft effect noise temperature	21						
Noise bandwidth	62	1.6MHz					
Boltzmann constant K	-228						
Pn = Noise Power KTB	-145						
Signal to noise ratio S/N	17	S/N = Pr/Pn= {Gt* Pt*l^2*Gr}/{(4*p*r)²*k*BRF*Lp*Ts}					

(MCU). The Enhanced Shock-Burst™ reduces system price when all the high-speed link layer operations are controlled.

The front-end of the radio uses Gaussian frequency shift keying (GFSK) modulation. Frequency-shift keying (FSK) is a frequency modulation scheme in which digital information is transmitted through discrete frequency changes of a carrier signal [45]. It has user configurable parameters like frequency channel, output power,

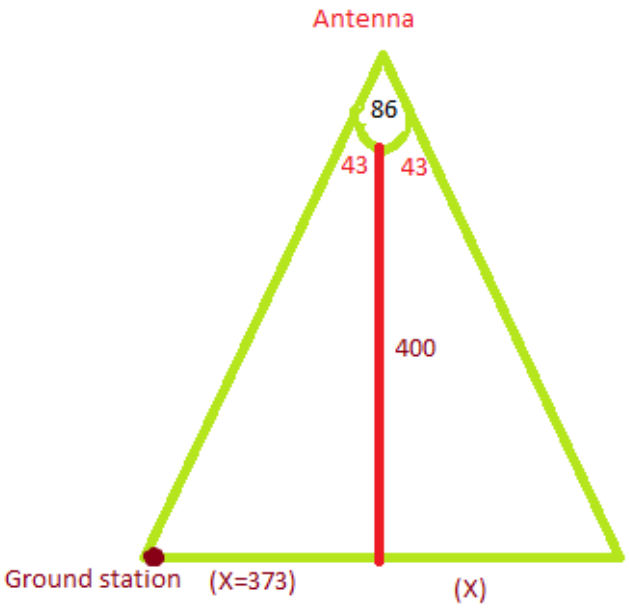

Figure 18: The distance calculated through the angle of the beamwidth to the antenna.

and air data rate. The air data rate supported by the nRF24L01 can be configured to 2 Mbps. The high air data rate combined with two power saving modes makes the nRF24L01 feasible for deficient power designs such as this work. The internal voltage regulators ensure a broad power supply range and a high Power Supply Rejection Ratio (PSRR). [46]

6.3 Communication Chip Layout

The communication chip layout is best understood through its various pin connection, and it is as follows. The 3 V voltage is supplied by the Raspberry Pi zero through its pin number 4, to the transceiver pin number 18. The pin number 3, 4, 5, 1 and 2 of this communication chip are connected to the Raspberry Pi zero SPI port, which is mentioned in the section concerning Raspberry pi zero.

The output from the transceiver is taken from the pin number 12 and 13. These pins are dedicated to antennas but connected through the PA and LNA. The output from these ports in the case of this project is first taken to an amplifier, and then this amplified output is supplied to the antenna. The schematic about the connections with the communications chip is presented in Figure 19, which shows all the connections necessary for the communication with transceiver chip to work under

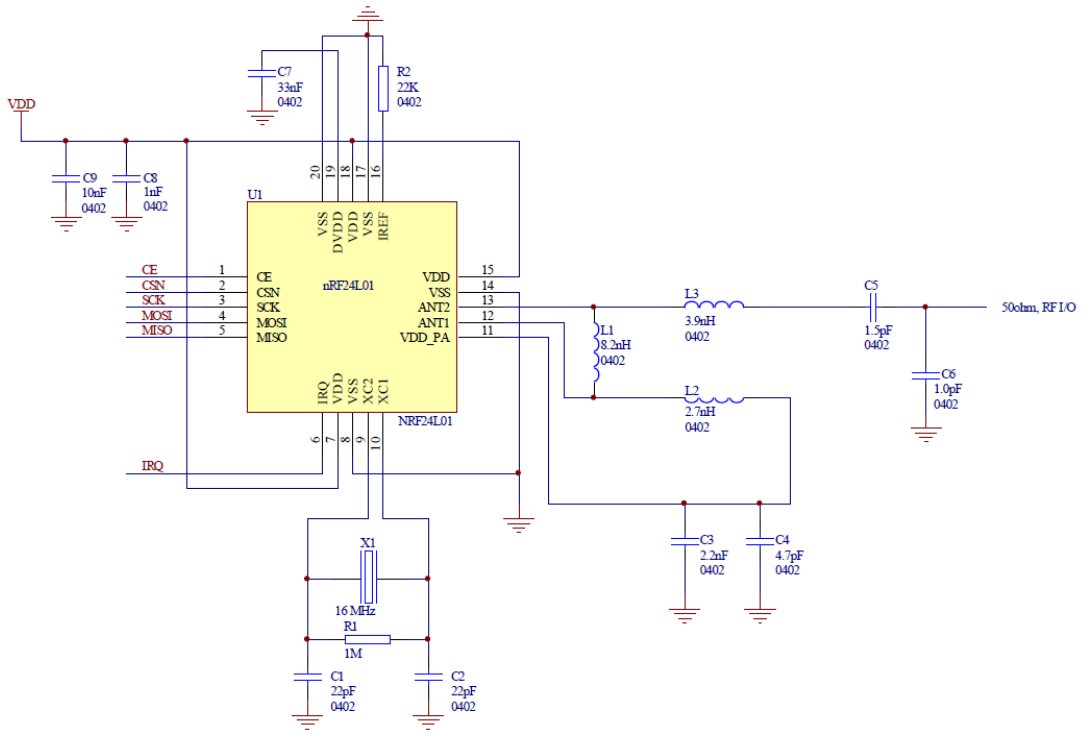

Figure 19: The connections necessary to connect the chip with other devices [46].

optimum conditions. The figure depicts that the pin from numbers 1 to 5 are left for the Serial port Interface (SPI) connection with the Raspberry Pi zero, while all other pins have been connected to different elements. The output from pin number 13 ANT2 is left for the RF connection with the patch antenna.

The communication chip also has PA (power amplification) in transmission (TX) mode. The highest value for PA is selected, which is 0 dBm or -30 dB. This value is still 30 dB less to reach the limit defined in the link budget, which is 0 dB. Therefore, before the output is supplied to the antenna, the power amplifier is required to boost the signal to the required limits.

The data rate of this communication chip can go up to 2 Mbps, yet the data rate for the communication is 256 Kbps to 1 Mbps, in order to avoid any interference or delay in communication.

In the receiving mode, there is one LNA (Low Noise Amplifier) used to receive a data rate of 1 Mbps and 2 Mbps at the sensitivities of -85 dBm and -82 dBm respectively. In Figure 20, two different modes of transceiver chip namely transmitting and receiving modes, can be observed. This figure highlights the PA (Power Amplifier) and LNA inside the transceiver chip, in which two different modes of communication are presented. The figure also shows various filters after the low noise amplifier, power amplifiers, the modulator, demodulator and the filter sections. The pinout of the chip can be shown in the Figure 21.

The pins of the chip are shown in Figure 21 and the order in which other devices can be attached. The black dot indicates the location of one number pin. The pin

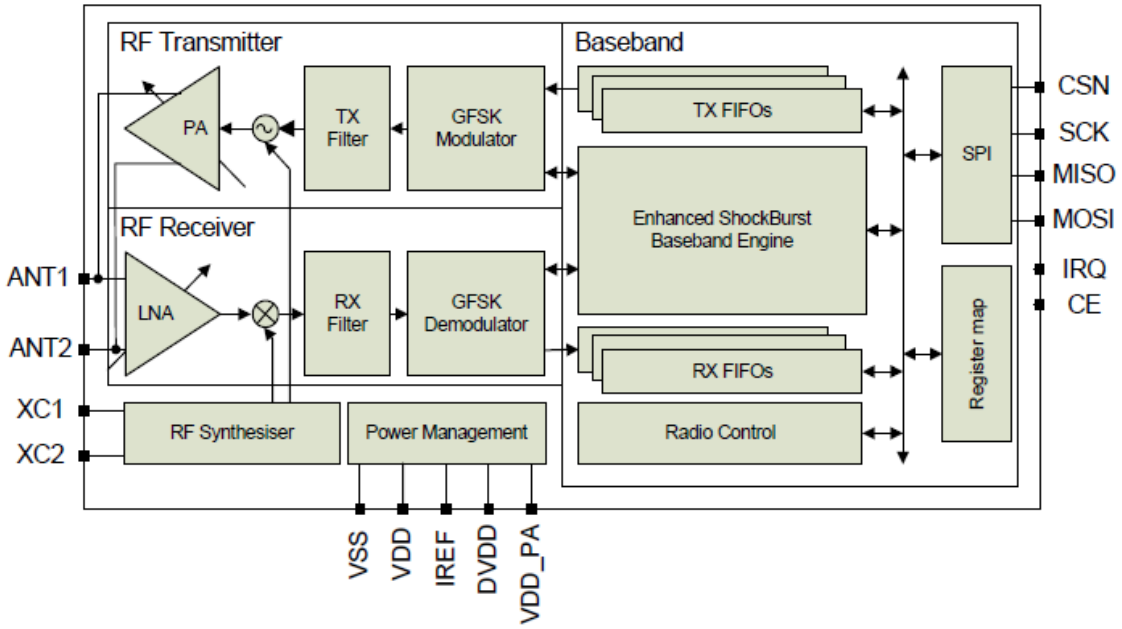

Figure 20: The internal structure of the nRF24L01 [46].

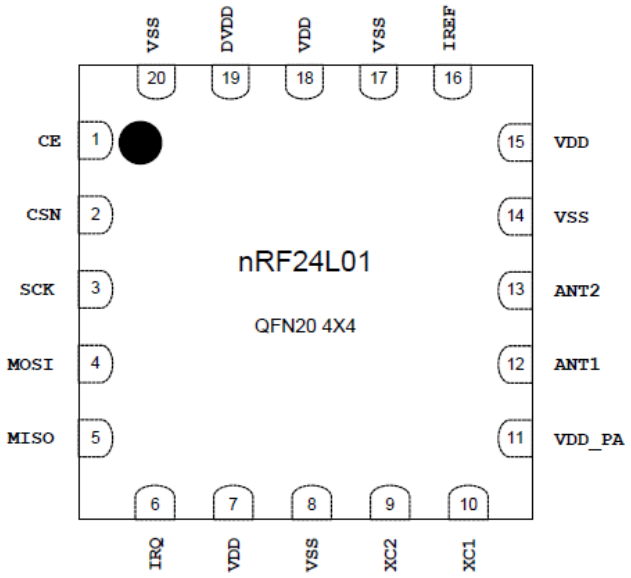

Figure 21: The pinout of the nRF24L01 [46].

number from 1 to 5 are the pins which are connected to the Raspberry Pi zero with the SPI (Serial Peripheral Interface) bus.

The power rating for the communication is lesser than the power rating of other similar transceiver chips, i.e., CC2500 [47] because with this communication chip only 12.3 mA is required for transmission mode. Power down rating for this chip is

900 nA and standby is 22 μA.

6.4 Power Amplifier

According to the values calculated from the power subsystem, to provide 1 W of power to the antenna, a power amplifier is needed after the communication chip in TX mode. This point is because the output power of the signal from the communication chip is only 0 dBm or -30 dB. Therefore, the signal coming from the communication chip needs to be boosted up to reach the limit of 1 W. For this reason, a power amplifier is needed which can provide amplification of 33 dB with low power requirements.

The power amplifier selected for the power amplification is the QPA5219 from Qorvo. The features of this chip are given below:

- Frequency Range: 2.4 GHz-2.5 GHz
- Output Power (POUT) = 24 dBm for Modulation and Coding Set (MCS) 8/9, Very High Throughput (VHT) 20/40, -35 dB Dynamic Error Vector Magnitude (EVM)
- POUT = 25 dBm MCS 7, High Throughput (HT)20, -30 dB Dynamic EVM
- POUT = 26 dBm 802.11 g, -28 dB Dynamic EVM
- POUT = 28.5 dBm 802.11b @ Spectral Mask Compliance
- Voltage = Optimized for +5 V Operation
- Gain = 32 dB Tx Gain
- Chip = Chip Integrated DC Power Detector
- Capability = MCS11 and 3.3 V Capable [48]

The Qorvo® QPA5219 is a three-stage power amplifier (PA) designed for the S-band. The integrated matching and firmly packed form factor reduce layout area in the application. Operation performance is focused on improving power consumption while the highest linear output power is stabilized. The design significantly reduced the external component needed, leading to a simplified board implementation and more steady performance at a system level over different conditions. The QPA5219 joins a 2 GHz power amplifier (PA), a regulator and a power detector for improved accuracy [48].

This PA works in the frequency range from 2.3 GHz to 2.7 GHz, and at the voltage range from 3 V to 5 V. This chip uses a low amount of quiescent current compared to the amplifiers of the same ratings. Another good point of this amplifier is that it uses a small amount of space on the board.

The maximum operating current for this PA is 500 mA to 600 mA with the optimized 5 V voltage. Space is less because its size is 3 mm $\times$ 3 mm compared to a

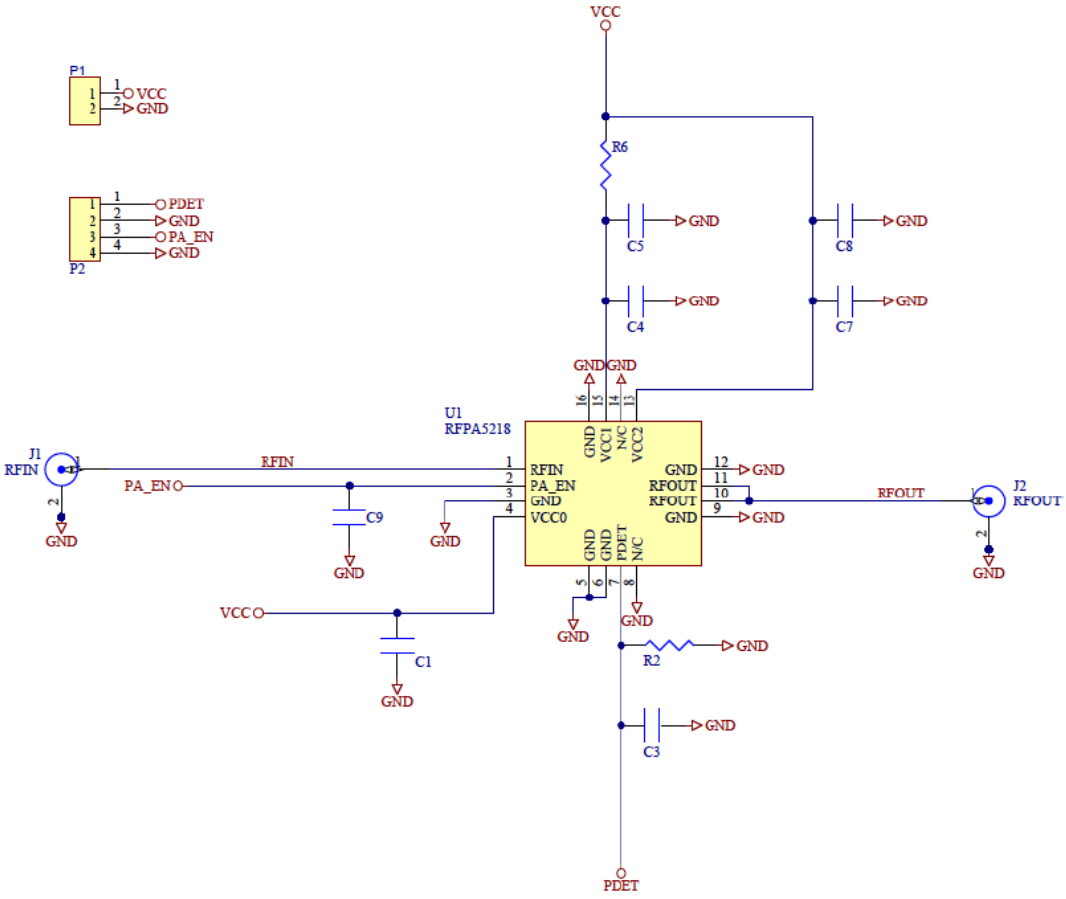

Figure 22: The number of components required for the 50 Ω matching circuit is displayed [48].

variety of PA's of the same frequency, and it uses fewer of components for a 50 Ω matching circuit. The 50 Ω reference circuit is shown in figure 22 which also points out on the different type of components connected to the PA in the Figure 22. The RFIN pin part attaches to the communication chip of the femtosatellite, and the RFOUT pin point of the PA connects to the antenna of the satellite.

There is also a PA enable pin to turn the voltage on and off. The internal functional block diagram explains the internal structure and its connection with different pins. The PA functional block diagram is shown in Figure 23.

The Figure 23 shows a connection between the input signal and the output of the chip. There is also a connection of a diode with a PDET (Power Detector) pin. This PDET pin is there to detect a low power signal and also to detect the exact voltage; the interference caused by the increase in the temperature is reduced by it.

6.5 Low Noise Amplifier

In this project, to increase the sensitivity of the receiver, a Low Noise Amplifier (LNA) is used. Although the transceiver has an internal LNA which raises the sensitivity

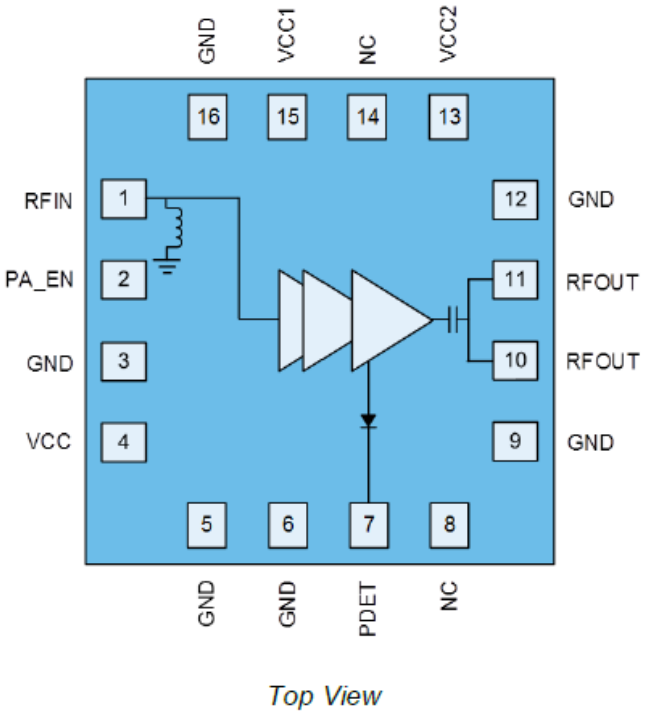

Figure 23: The the functional block diagram of the QPA5219 [48].

up to -85 dBm at 1 Mbps, with this external LNA the sensitivity of the receiver was further raised. The sensitivity was increased due to all the noise and attenuation from the ground station to the satellite in LEO orbit, such as mismatching in the receiver, polarization losses, and misalignment losses.

The LNA selected for the femtosatellite is the SST12LN01 from Microchip [49]. This amplifier was selected because of low energy requirements, smaller size, less amount of components for the circuit, very straightforward design requirements and the high gain qualities of the chip designed for the frequency between 2.4 GHz to 2.5 GHz.

According to the product description, the SST12LN01 requires no rf matching components. This device complies with 802.11 b/g applications and is based on GaAs pseudomorphic high electron mobility transistor (pHEMT) technology. The SST12LN01 provides low noise, high performance, and moderate gain operation for the frequency of the 2.4 GHz to 2.5 GHz band. Around this frequency range, the LNA typically provides 13.5 dB gain and 1.5 dB noise figure [49].

This LNA cell nominally at ten mA during operation retains has low DC consumption, which is designed with is a self-DC biasing operation. Optimum performance is accomplished with no external bias resistor or networks needed and only a single power supply. The input and output ports are single-ended 50 Ω matched. The rf ports are also DC isolated, so no DC blocking capacitors are required or matching components. The SST12LN01 is offered in 6 contact ultrathin quad flat no-leads (UQFN) package. [49]

The LNA is preferred over others, because of the qualities given in the product

description that it requires a low number of components for rf matching, has low DC consumption, and self-DC biasing over the frequency range of 2.4 GHz-2.5 GHz that makes it suitable for femtosatellite.

The six-contact UQFN package is the other point which makes it more favorable over other LNAs available on the market. The Lower contact package accounts for a fewer number of components used and the relative simplicity of the package. The simplistic package is also significant because it requires no programming for the chips. The UQFN package is shown in Figure 24. In Figure 24, it can be seen that only

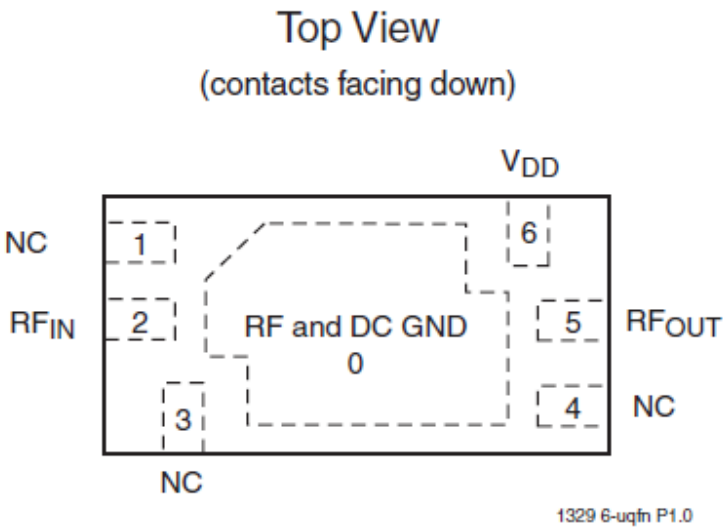

Figure 24: The top view showing all the contact point of LNA [49].

three of the six contacts are necessary which are Rfin, Rfout, and VDD. The other contacts can just be left unconnected, meaning that the space for the circuit is saved. The reference design of the LNA for the different application circuits is shown in Figure 25 which shows that only one 0.1 μF capacitor is needed to use this LNA, which makes the present LNA suitable for the satellite. The resistors are connected to the Rfin and the Rfout contacts of the LNA to show that they are matched with 50 Ω resistance, and the capacitor is added to the Vdd contact of the chip.

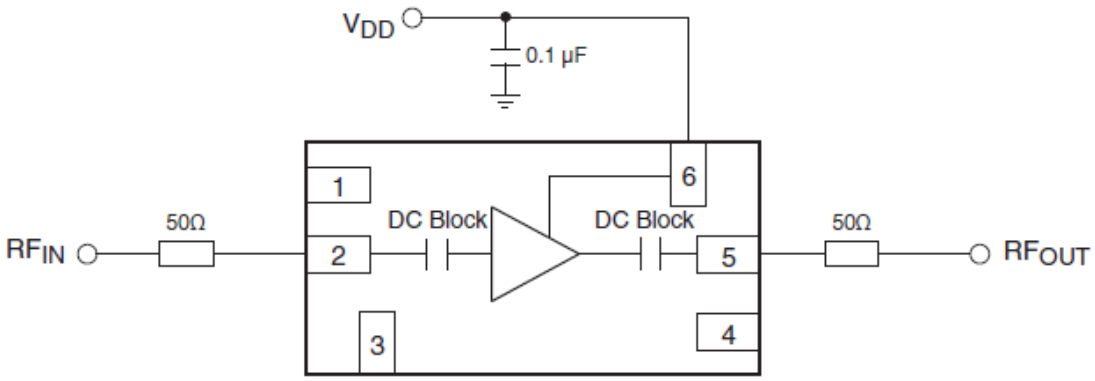

Figure 25: The components required for a typical application circuit with this LNA [49].

7 Attitude Control of satellite

Attitude control is the control of the orientation of satellite according to the inertial frame of reference. There are different kinds of small satellites each having different mission types; most satellites use different kinds of antennas to point out their location to the ground station. Recent satellites have novel technologies with directive [50] narrow-beam antennas, in which tight pointing accuracies are required to ensure adequate communication. Therefore, there is a constant need for an attitude control system for satellites with a spin or three-axes stabilized system with 1 degree or less pointing accuracies.

The selection of an attitude control system (ACS) is a function of many factors including mission objectives, orbit, and the available system budgets such as link and mass budgets. The stabilization systems in which momentum and reaction wheels are used as control torque sources are suitable for small satellite applications due to their proven performance, relative simplicity, versatility, and their capability to provide high accuracy pointing control [51], However, for femtosatellites, such stabilization systems are still in the category of high mass.

There are two types of torquers: active and passive. The passive torquers are systems which include permanent magnets that interact with Earth's magnetic field to move the satellite. For femtosatellites, there are different active control torquers which have low weight, and their types include systems like use Electric tethers [52], Micro Control Moment Gyroscope [53] and low weight torquers which help the satellite to move.

Magnetometers also form part of the attitude control system in the satellite. These magnetometers perform a specific function in the satellite's attitude and control system: for instance, in the way they help satellite to be aware of its attitude when the strength of the magnetic field is calculated [54] and then the satellite can be controlled through active control.

It is necessary to know the magnetic field around the satellite for attitude stabilization. Minimal weight, size, and power consumption are the most critical properties of a control system. The magnetic flux can be measured in 8-bit resolution [55]. Furthermore, the feasibility of active attitude detection and active attitude control can be checked in the coming sections.

Some options for active attitude control are studied and are checked for suitability. One such example of active control is a Sun tracker of the type "nanoSSOC-A60". Since a femtosatellite has been proposed in which a directive antenna is used, the payload of a video camera and antenna are pointing towards Earth while the solar panel is directed towards the sun. This type of device uses low power and possesses low mass and will suit best for a femtosatellite but still, it adds some weight in the satellite.
The specifications are as follow:

- Type = 2 orthogonal axis
- Field of View = $\pm$ 60°

- Accuracy = $< 0.5°$ (3sigma), $< 0.1°$ (precision)
- Electrical interface = 4 voltage outputs, 10-pin micro-connector
- Power supply = 3.3 V / 5 V, $<$ 2 mA consumption
- Mechanical interface = 27.4 mm $\times$ 14 mm $\times$ 5.9 mm, 4 g
- Housing Aluminum = 6082, Black anodizing [56].

Different options for the magnetorquer were studied. For the purpose of direction control and tumbling control, three magnetorquers are needed inside the satellite. These three are for control of the pitch, row and yaw movements, and they should be placed under the solar cells and in the space between the PCBs.
Instead of commercially buying the magnetorquers, one option was to make them at Aalto University.

There is also an option that a MEMS gyroscope should be used for the tumbling detection because of its low mass properties. A gyroscope is a device in which a wheel or disc mounter is present so that it can rotate or spin fast around its axis which is itself free to change in direction. The orientation of the axis is not affected by tilting or rotating of the mounting, so gyroscopes can be used to provide pointing or maintain a reference direction in navigation systems, automatic pilots, and stabilizers.

The presented MEMS gyroscope weights 2 to 4 g, the power requirement is also low, and the model of the gyroscope is ADXRS290 [57]. However, magnetometers and magnetorqures add mass in units of tens of grams, so these are above the weight limit; therefore, the permanent magnet can be used to point the orientation of the satellite.

7.1 Attitude Control Design

A different design for the attitude control system is presented in this section unlike the system with magnetorqurers or magnetometers.

Most of the active control system includes magnetorquers, reaction wheels, and ion propulsion systems. These parts are manufactured to the CubeSat (nanosatellite) scale level. Therefore, they are much bulkier for the femtosatellite level and require much power compared to what is feasible at femtosatellite level.

The option of self-made active control components such as magnetorquers is fine and feasible, but the weight of the components remains problematic for the weight limit at the femtosatellite level. Therefore, the active control is not a practical solution for a femtosatellite unless some innovative idea is put forward to change this situation.

The solution presented is a passive control system, which relies on the magnetic field of Earth. Since the magnetic field is not the same over different regions of the world, there is much variation in the magnitude as well as in the orientation of the field. Therefore, the solution presented in this work takes in to account the anomalies of the varying magnetic field of Earth. In Figure 26, a detailed view of the Earth magnetic field is shown. The Figure 26 shows the magnetic field orientation of

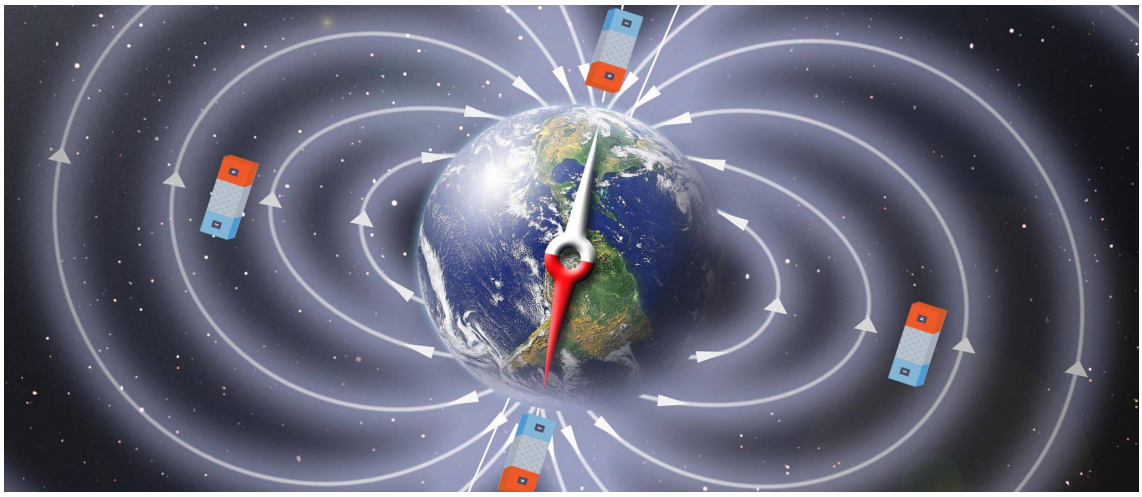

Figure 26: The orientation of magnetic waves around the surface of the earth.

different parts of Earth. Such information helps when a permanent magnet is placed on the satellite to rotate in the desired direction.

In this attitude control system design, there is no need for any magnetometers because the system is a passive control system. According to the International Geomagnetic Reference Field (IGRF), which is a standard mathematical description of the large-scale structure of the Earth's main magnetic field and its secular variation. Earth's Magnetic Field strength at the altitude of 400 km (over Espoo Finland) is 43880.2 nT, and it is pointing downwards towards Earth. The site mentioned is where the ground station is located in the present work. In the Figure 27 calculation made by the IGRF can be seen [58].

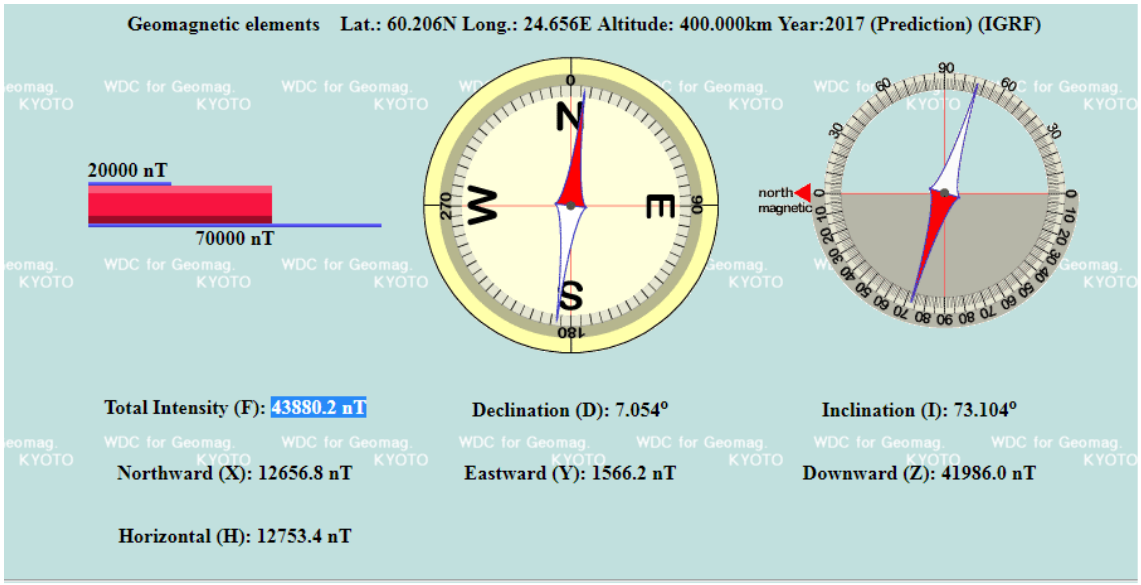

Figure 27: Different aspects of Earth's magnetic field over the desired Earth's magnetic field region in Espoo Finland [58].

Figure 27 depicts the main features of the magnetic field of Earth-like such as total intensity, declination, inclination, and direction of the magnetic field. It is seen that the compass needle in the figure is pointing towards the north of Earth and shows a declination of 7.054 °. The second compass shows an Inclination of 73.104 °.

To work with this magnetic field, a disc magnet Ø 15 mm with a height of 8 mm was selected from Supermagnete. This magnet is only 11 grams with the strength of approximately 6.7 kg, which makes it a passive control system. It is Nickel plated and has the magnetization of N42. Some other features of this magnet are listed below:

- Used Material: NdFeB
- Shape of Magnet: Disc
- Diameter of Magnet: 15 mm
- Height of Magnet: 8 mm
- Tolerance level: +/- 0.1 mm
- Direction of magnetization: axial (parallel to height)
- Coating: Nickel-plated (Ni-Cu-Ni)
- Magnetization: N42
- Approx. strength: 6.7 kg (approx. 65.7 N)
- Maximum working temperature: 80°C
- Total Weight: 11 g [59].

8 On Board Computer(OBC)

The on-Board Computer is, as the name suggests, somewhat naturally, the computing part of any unit flying on board a satellite or a rocket. It is a small computer capable of doing a different sort of tasks related to the computer in the orbit of the satellite.

For the OBC there is also an On-Board Software (OBSW) which is predefined and present in the computer. The "On Board Software," despite the somewhat generic title, is known for the software running the satellite's vital functions such as attitude and orbit control in both nominal and non-nominal cases. Its functionality includes onboard time synchronization and distribution, failure detection, isolation and recovery, telecommands execution or dispatching, housekeeping telemetry gathering, and formatting, and so forth [60].

The control of the platform is mainly implemented by the functionality of OBSW and the operational flexibility from the ground station. The performance of the OBC is based on the performance of the OBC architecture and hardware. Therefore, the chain of operations held in the spacecraft is controlled by the complementing software, and defining the architecture of the whole system based on both OBC and OBSW is an engineering challenge [61].

The platform of the satellite was controlled by one OBC, and the payload was controlled by a separate OBC in the older satellites, but in the newer satellite, the platform, payload and all the components of the satellites are controlled by only a single OBC [61].

The central subsystem which runs the satellite regarding operations and handling, the OBC, can be designed in different ways. The different factors that affect the satellite function and the performance of the OBC vary from those of a terrestrial computer; therefore the satellite design of the OBC is significantly different from the terrestrial computer [62].

8.1 On-Board Computer Design

A Raspberry pi zero board with 1GHz ARM11 core was selected for the onboard computer and all the connections with other components. This PCB board was chosen because of its low weight and low space taking qualities, which is the requirement for a femtosatellite. The board also includes ports and connection points to connect different components with them, which is an ideal quality for a small satellite.

The Raspberry pi weights 9 grams, and a small form factor of 6 cm makes it a good component through which good computancy is achieved with the smallest form factor. Other mentionable capabilities which it possesses are as follows:

- A Broadcom BCM2835 application processor
- 1GHz ARM11 core
- 512MB of LPDDR2 SDRAM
- A micro-SD card slot

- A mini-HDMI (High Definition Media Interface) socket for 1080p video output
- Micro-USB sockets for data and power
- An unpopulated 40-pin GPIO (General purpose Input Output) header
- Composite video and reset headers
- Camera Serial Interface (CSI) camera connector (v1.3 only)
- An unpopulated composite video header
- Smallest ever form factor for Raspberry Pi, at 65 mm × 30 mm × 5 mm [63].

The forty pin GPIO header is also capable of providing other connections such as SPI, Integrated Circuits (I2C) and Universal Asynchronous Receiver-Transmitter (UART) ports. Therefore, this provides ease for the connection with different parts, i.e., the transmitter, LNA, and Camera. The GPIO header also includes ports to provide power to those connections. In Figure 28 the Raspberry pi zero is shown with different components.

Figure 28: All the components and the pinouts for attaching different component with it [63].

Figure 28 also shows two small USB ports (one can be used for power and the other for data), a card reading port on one side, a camera CSI port on another side, a processor and a HDMI port.

On the left side of the Raspberry Pi zero, there is a forty-pin GPIO, with which different components are attached. These forty pins have different functionalities and have different positions on the forty pin GPIO header. The pins on the header are arranged, and the header arrangement is provided to ensure the pins are used in the correct order. The GPIO Pin Header of the Raspberry Pi Zero is shown in Figure 29 which presents different pin positions, for instance, pin numbers 1, 2, 4

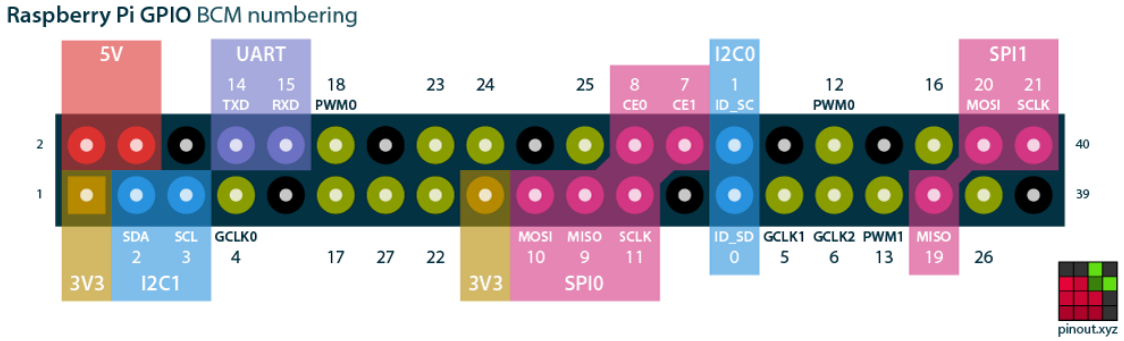

Figure 29: A comprehensive layout of Raspberry pi zero pinout [64].

and 24 relate to power, 3, 5, 27 and 28 are for the I2C, 19, 21, 23, 24 and 26 are for the SPI connections, 8 and 10 are for the UART connections and the remaining pins are all GPIO pins.

According to this work, power in the design of the femtosatellite for the Raspberry Pi is provided through the Micro-USB socket. All the SPI pins which are 19, 21, 23, 24, and 26 are used to transfer data between the Raspberry Pi zero and the communication chip nRF24L01. These pins are respectively connected to the 3, 4, 5, 1 and 2 number pins of the communication chip.

The Master Output Slave Input (MOSI), the Master Input Slave Output (MISO) and the Serial Clock (SCLK) are the first three SPI pins, and Chip Selects (CE0 and CE1) are the last two pins which are connected between the Raspberry Pi zero and the communication chip.

Pin number one that supplies power provides 3 volts voltage to the communication chip. It also provides power to a power amplifier from pin number 4, which in return provide amplified output to the antenna.

9 Payload

An Earth Observation (EO) satellite can be conceived as being composed of two separate parts: the platform and the payload. The platform is synonymous with the chassis of a car: it is a frame on which other components can be attached. The platform typically also includes all the necessary infrastructure required to do the whole satellite work, including the solar panels, the batteries, the onboard computer, the memory banks, the communication modules, and antennas, and so forth.

By contrast, the payload includes all the components and other devices that generate the EO data or the associated metadata. Each satellite has a specific payload, and lots of examples of payloads are found by visiting the websites of specific instruments on past and current platforms. Some examples of payload on the internet are AVHRR, Landsat, SPOT, Pleiades, WorldView, MODIS, MISR, MERIS, SeaWiFS, and Sentinel [65]. The payload defines the functionality and purpose of the satellite. If the payload is for a video recording purpose or sending images from space, then a camera is the required payload.

Sending images of earth from LEO orbit is the main function of this femtosatellite project. There are two ways for that: one is remote sensing, and in-second images are taken by a camera. However, it has been noted in satellites that use of remote sensing payload makes satellites heavy and also the remote sensing instrument consumes much power.

The percentage of payload weight of different remote sensing satellites is drawn concerning the total satellite weight. It is observed that 10%–50% of the satellite weight is allocated to its payload. The same goes for power consumption as well [66].

Here the payload of a camera is discussed. There are different types of cameras used in a satellite mission from which good quality images are provided, i.e., narrow-angle camera, wide-angle camera, photopolarimeter systems, and so forth.

As for getting the data, the data is transmitted back to Earth and is received by NASA's Deep Space Network of radio dishes placed around the world specifically to receive transmissions from various space probes out in the solar system. The rates are low by today's standards, but this is technology dating back to the late 1960s and early 1970s. For example, Voyager telemetry operates at these transmission rates:

- 7200, 1400 bit/s tape recorder playbacks
- 600 bit/s real-time fields, particles, and waves; full Ultra-Violet Spectrometer (UVS); engineering
- 160 bit/s real-time fields, particles, and waves; UVS subset; engineering
- 40 bit/s real-time engineering data, no science data.

So the best transmission rate is only 7.2 kilobits per second for voyager [67]. The example of voyager was chosen, although it is not EO satellite but because to show that data can be received from the ends of our Solar system.

There is also a problem that concerns the required power to send those high-quality images back to the ground station; therefore, camera quality depends on the

power and mass required for the satellite. In the case of a femtosatellite, the camera size and power limitation have to be prioritized and given importance aside from image resolution. Here is one example of the camera for the small satellite.

The specifications are as follows:

- Idle power: 0.1 mA
- Max. Power: 150 mA
- Resolution: 1280 × 1024
- Rate: 15 fps
- Temperature range: −20°C to 60°C [3].

9.1 Camera Payload

Satellites use different types of cameras to capture images. These cameras record visible light to produce images. Other types of cameras use infrared light to measure heat signatures. This feature allows geographers to map more extensive areas of Earth and they can be used in world weather, to measure ocean temperatures.

For the selection of the payload camera, two requirements were to be met, the first was the low weight of the component required for the femtosatellite project and the second was the low power requirement also derived from the requirements of the femtosatellite. Camera size has also to be taken into consideration because board size and connections with the main board can affect the structure of the satellite.

According to these requirements, there are many small cameras available on the market from different companies with different functionalities and resolutions. The camera should have resolution according to the data rate defined by the communication subsystem. This requirement is because the resolution has to be less than or equal to the data rate defined by the communication subsystem; otherwise, it will take either days or even weeks to acquire images from satellites.

Therefore, the camera resolution has to be according to the data rate, so the images can be accessed when the communication link with the satellite has been established. For this reason, the camera selected for the femtosatellite is the Raspberry camera v2.1 with the mount. This camera is an 8-megapixel camera with a Sony IMX219 image sensor, which comes in the custom designed board. This camera was selected because the total weight of this camera with a board is merely 3 grams which is a significant advantage for a femtosatellite. Moreover, the camera was selected because of its compatibility with the Raspberry Pi zero, which is the on-board computer for this femtosatellite.

The camera has fixed focus, capable of 3280 × 2464 pixel(p) static images, and also supports 1080 p, 720 p, and 640x480 p video, so if the femtosatellite is not able to have a good enough data rate, then the resolution can always switch to a lower level.

This camera attaches to the Raspberry Pi zero with the help of a small socket on the board. The socket used to connect is the CSI. In Figure 30 the camera with a CSI connector can be seen.

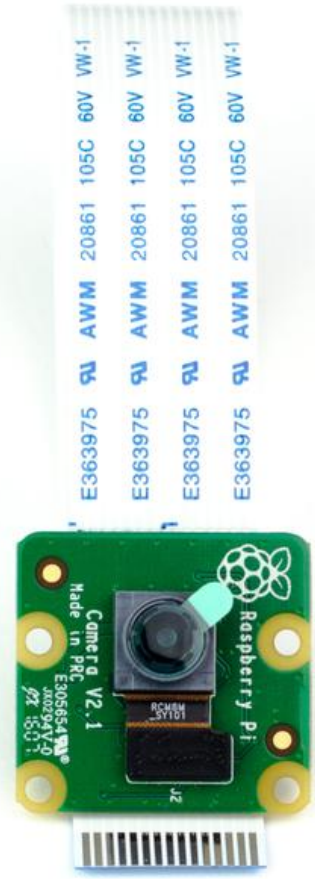

Figure 30: Camera that can be connected with the Raspberry pi zero with the help of CSI connector [68].

There are a few other features of this camera which can be listed as:

- Fixed focus lens on-board
- 8 megapixel native resolution sensor-capable of 3280 × 2464 pixel static images
- Supports 1080 p, 720 p and 640 × 480 p video
- Size 25 mm × 23 mm × 9 mm
- Weight just over 3 g
- Connects to the Raspberry Pi board via a short ribbon cable

- Camera v2 is supported in the latest version of Raspbian, Raspberry Pi's preferred operating system [68].

This camera can also fit easily in the commercially available structure of the femtosatellite, discussed in chapter 10, structure of the femtosatellite. In Figure 31, the camera inside the proposed structure is shown.

Figure 31: Camera can be easily fitted inside the structure proposed for the femtosatellite [69].

10 Structure of Satellite

The structure of the satellite is also a vital part of satellite manufacture, and it should be taken into account when the components for the satellite are chosen. This structure not only protects the satellite from damaging temperatures but also shelters the satellite from objects in space, space plasma and also in case of vibrations in the satellite.

In the case of the femtosatellite low-cost solution, short development cycles, the maximum degree of freedom in the sense of structural concepts, payload and board placement, and the ability of the satellite to withhold several launches by making several affordable copies of the first, are good points for structure development.

Structure development is the long and complicated process where the material for the satellite that concerns heat protection and suitability with the satellite is selected, and the structure is made in such a way that would accommodate different subsystems each with different requirement. The structure also needs to have several electrical and data paths for different subsystems.

According to a study on the structure of small satellites which suggests that small satellites should have modular structures. Modularity has brought advantage to the design and analysis of S/C (Spacecraft) structures. A designer may take full advantage of parametric and standard design components. An analyst can use verified hand-calculation methods or tested FE (Finite Elements) methods. The study gives confidence that the selected common elements are well suited to be used in small modular satellites [70].

In one example a packager and orbital deployer were customized to integrate with the standardized CubeSat dimensions. The standardized structure covered a femtosatellite in one case. This structure was done by ASU(Arizona State University) students [16].

In other cases, it is just engulfed between pieces of PCB such as the Wikisat group by Tristancho [3]. The material for the package type in the ASU satellite design is aluminum, and for the Wikisat material is FR-4.

The temperature ranges for the LEO orbit at 400 km are from -156 °C to 121 °C [71] which are above the temperature ratings at Earth and are dealt with by using kevlar shielding. Therefore, mainly the structure serves as a temperature protective material in this work for a femtosatellite. Most of these materials in this work have temperature ranges that are able to withstand temperatures around 80 °C and also a little below -20 °C.

10.1 Commercially Available Structure

In order to know the specifications and type of material that should be used for structure, the time femtosatellite spends in sunlight needs to be found out. The orbital time calculation is as follow, the radius of Earth is known which is 6371 km, and the velocity calculated in the link budget as 7.7 km/s. At this distance, the 400 km orbit is added. The values are taken through Newton's form of Kepler's third

law; we can calculate the period the satellite spends in orbit. The law is as follow:

$$T^2 = \frac{4\pi^2 r^3}{G m_{Earth}}, \tag{7}$$

where T is the period of the satellite, r is the radius of Earth, G is the gravitational constant, and m_{Earth} is the mass of Earth.

Equation 7 gives the values the value of 92.45 minutes for the period of the orbit. The time it spends in the sunlit area or shadow area can damage the components of satellite. Therefore, femtosatellite with this orbit period, still needs a structure to cover it from heating and cooling damages during these periods.

For the structure of the femtosatellite, commercially made structures are available precisely according to the OBC of this satellite, and it is spacious enough to contain all the components of this femtosatellite. The commercially available part of the structure of the femtosatellite is the Pi Foundation Raspberry Pi Zero case which is chosen because of its compatibility with the Raspberry Pi zero board. This mainboard is the on-board computer for this femtosatellite. It not only provides the suitable space for the Raspberry Pi zero board but it also has extra space to engulf other parts of the femtosatellite. This covering is made of plastic which can shield it from hazardous temperature for the satellite. The manufacturer, however, doesn't provide any detail of which kind of plastic it is made of. If the plastic cover from the manufacturer is not suitable in space, then different type of material can be used like aluminum or kevlar shielding can be used. In Figure 32 the picture of the covering is shown.

This cover also has a small hole in the middle to provide an opening for the camera of the satellite which eliminates the need to put the camera outside the covering to protect it from heat.

On this product, there is also room for the placement of the solar cells on both the top and the bottom part of this covering. There is also a place for the antenna on the top side near the camera hole to avoid any interference from the cover, but it can also be placed inside.

There is enough space on this cover besides the Raspberry pi zero board: that space can be used for the communication circuit design and other necessary parts of this femtosatellite. Figure 33 illustrates the internal space for the pi zero cover for this femtosatellite.

Here are some technical details of this product:

- Case Dimensions: 79 mm × 38 mm × 15 mm
- Case Weight: 14.4 g
- Camera Cable Length: 38 mm

About the material of this case, which is made of an unspecified plastic, if this plastic is of the type which is not suitable to be used in space, then the case can be made with machined aluminum. It has the same dimensions which are 79 mm ×

Figure 32: The structure of commercially available cover for Raspberry Pi zero [69].

38 mm × 15 mm with the thickness of 0.08 mm. The mass calculated from these dimensions for an aluminum casing is around 16 g.

The aluminum cover can also be modified according to changes in the structure or if more components are added to the femtosatellite. The solar cells and antenna are placed on the outer surface of the cover.

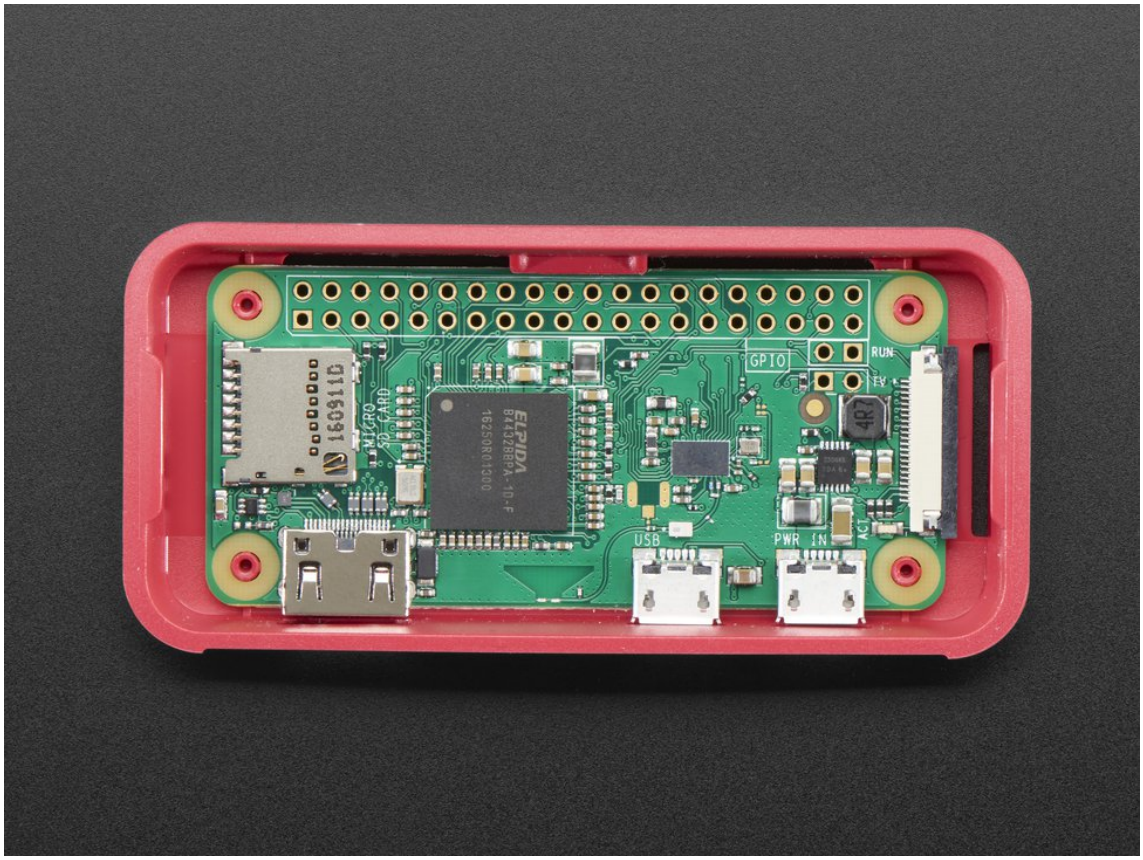

Figure 33: The internal space of the femtosatellite cover [69].

11 Internal Design of Femtosatellite

Different parts of the femtosatellite and their interaction with each other are focused on this part, and the internal design of the femtosatellite is stated. The power and the data that is transferred to different parts of the satellite is also presented.

11.1 Block Diagram

This section is based on the block diagram and schematic design of the femtosatellite. There are three main parts of this internal design: the first is the power section, the second is the communication part of the design and the last part points out the payload and other parts.

In Figure 34, the block diagram for the internal design is presented, which describes all three parts of the internal design.

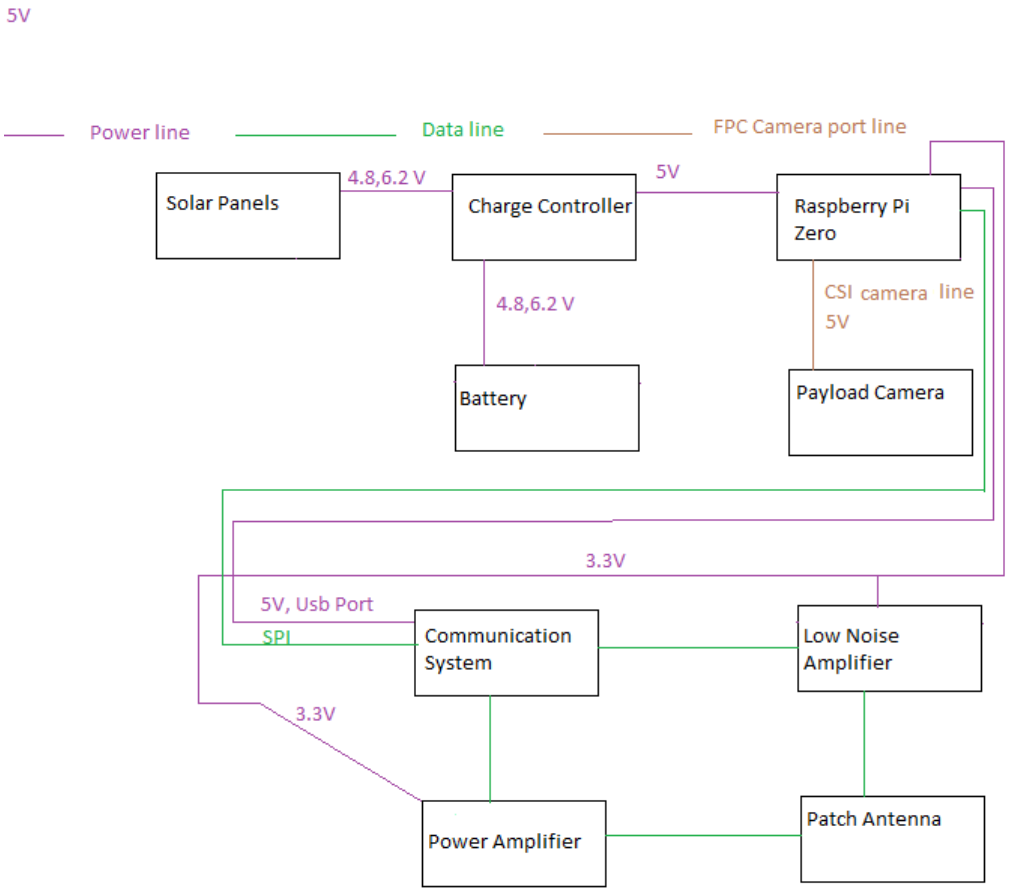

Figure 34: Block diagram of the femtosatellite and different connections between the parts of the Femtosatellite.

The central parts of the femtosatellite are indicated in Figure 34. The first

three block shows all the main components of power subsystem which are the Solar Panels, the charge controller, and the Battery. The OBC and Payload parts are illustrated by the Rasberry Pi zero and Camera block respectively. The last four blocks constitute the communication part of the design, which has the transceiver in the communication block. On the bottom side, there is a Low Noise Amplifier, a Power Amplifier and a Patch Antenna in subsequent last three blocks.

Different colored lines indicate the difference in nature of the supplied information through the lines, that is mentioned in Figure 34. The purple ones are the power lines, while green and brown are data and CSI port(which also provides power) lines respectively.

In the block diagram, it is shown that the OBC is connected to almost all the parts of the femtosatellite except for the Patch Antenna, Solar Cells, and the Battery. The parts which have no connection with the OBC are those parts which do not require any active control from the OBC.

11.2 Schematic

The detailed view of the internal structure of the femtosatellite is presented in the Figure 35 through a schematic, in which all the components like the resistors, capacitors and crystal oscillator etc, are included.

Figure 35 is the schematic for all the subsystems of the femtosatellite except for the permanent magnet and payload. This detailed schematic starts from the Raspberry Pi zero which is on the bottom-left-side of the schematic; this is the OBC or the control center of the femtosatellite. These connections of this OBC go to every subsystem of the femtosatellite, which can be seen in the schematic.

After the Raspberry Pi Zero, the next major component in the schematic is the transceiver, which is connected to the OBC via the SPI ports. Different types of components are connected to the device like a resistor, capacitor, oscillator, etc. to have a 50 Ω matching network.

The transceiver then connects to the PA and LNA through two switches of the same type. The switches are of the Skyworks type AS193-73, and they work on 2.4 to 2.5 GHz frequency. These are electronic switches, which are controlled through the OBC. These switches control whether the input from the transceiver should go to the PA or the output from the antenna should come through the LNA.

In the schematic, after the switches, there are two different amplifiers: the PA and the LNA. The PA takes the input from the transceiver via the switch, and the PA is also matched to 50 Ω. The power to the PA is provided through the Raspberry Pi Zero. The amplified output from the PA goes to the antenna through the switch.

The other component attached to the transceiver via the switch is the LNA. The LNA takes input from the antenna through the switch, which can be seen in the top rightmost corner of the schematic. The LNA then sends the amplified input from the antenna to the transceiver. These switches take power from the GPIO ports of the OBC. The PA and the LNA both take power from the OBC.

This section concludes the communication part of the femtosatellite, in which all components are matched to 50 Ω. The OBC connects with the payload camera to

send or receive images through this communication part of the femtosatellite. The payload is not shown in this schematic.

Under the communication components of the femtosatellite, the power section of the femtosatellite is placed. There are three components of this section, which are the solar cell, battery, and the controller of the femtosatellite. These are connected with each other to supply power to the femtosatellite through the OBC.

The solar cell is connected to two components. One is the battery for the femtosatellite, and the other is the charge controller. They are not connected to the OBC because they are passive and they need not be controlled. The reason for connection with two components is that if the charge controller cannot draw power from the solar panels, the battery will provide stored power. The battery is attached to two components, which are the solar cell and the charge controller. It is also not controlled by the OBC.

The last component in this chain is the charge controller of the femtosatellite. The charge controller receives power from both the battery and the solar cell. From the charge controller, the power is provided to the OBC after it is regulated and collected through the solar cells or battery.

The charge controller of the femtosatellite in this schematic is not of the schematic level, but it is a PCB level diagram. However, because to make the schematic inclusive of all components, it was done so.

Discussion on the schematic is not complete without the Mass and Power budget of the femtosatellite. That is a necessary detail to keep the design within the bounds of the thesis requirements.

11.3 Mass and Power Budget

The mass and power budget, as the named suggests, calculates the mass and power requirement for the whole system. It is made up of the mass and power requirement of each subsystem present and is compared to the satellite with the requirements.

With the help of the mass and power budget, the acquirement or removal of subsystems due to any increase or decrease of mass and power can be done. This budget planning plays a useful role in the whole makeup of the system. In the mass and power budget, Table 3, the highest rated values of the components were taken to increase the flexibility of the budget.

The available power is more than 1 W, but for flexibility of the budget, 1 W output power from the solar panels was presented.

Table 3: Proposed Mass and Power budget

Power and Mass Budget						
Components	Mass(g)	With Margin	Power(mW)	Idle power(mW)	Temparature Range©	
					Min	Max
Battery 4.5 Wh	23	27,6	0	0	-10	45
EPS	10	12	2		-40	85
Solar panels	2	2,4	0	0	-40	85
structure	15	18	0	0		660
Magnet	11	13,2	0		-35	75
Radio+OBC	15	18	800	4	-40	85
Antenna	5	6	0			135
Payload	5	6	75		-20	60
	86	103,2	877			

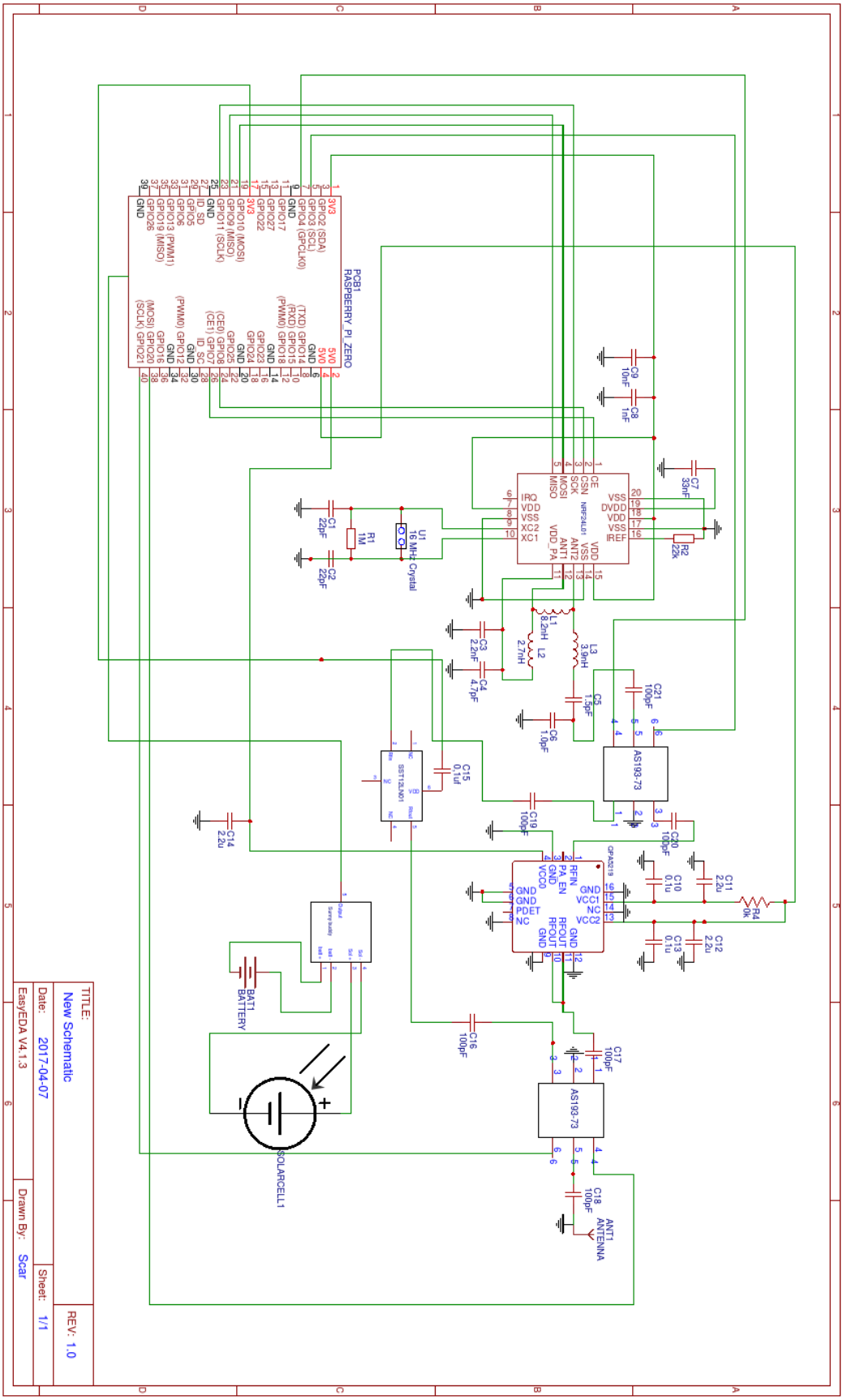

Figure 35: The schematic of femtosatellite

12 Conclusions

In Conclusion, it can be said that the design of this 100-gram femtosatellite points out that this kind of satellite is not only physically possible, but it is cost effective as well.

The femtosatellite link budget unfolds that it is possible that this type of satellite can communicate through the commercially available transceiver and circular patch antenna on the satellite, with a parabolic antenna on the ground station.

From the cost analysis of the whole subsystem, it can be concluded that in this concept of the femtosatellite, it is less expensive than its massive predecessors. Moreover, the low amount of weight allows it to have minimum number of components.

This femtosatellite design shows that it can send images, on request from the ground station. Images are taken with a camera and sent through the high data rate communication system with the directive antenna. This satellite will hold space for other types of lightweight payloads as well as for sensors.

The design of this femtosatellite allows it to have a weight of around 100 grams, and the power used by the satellite is also less than power produced and stored in the battery. This is present in the power and mass budget table 3 of this thesis.

In the view of this design, it can be said that this kind of satellite would be suitable for LEO orbit of 500 km or lower, depending on how suitable the communication subsystem of that satellite is and what type of payload issued.

The design of this femtosatellite manifests that it is possible to make a femto-class satellite with commercially available parts. Most of the parts in this femtosatellite were commercially available down to chip-level except for a few parts such as the antenna.

For future work on the femtosatellite, the antenna for this satellite should be modified from a directive antenna to an omnidirectional antenna. So that this antenna does not have any restriction, that it can only communicate when it is pointing towards the ground station with a future battery technology that have enough storage capacity for a whole femtosatellite operation period.

One modification is to replace the permanent magnet with a light-weight magnetorquer because the magnetorquers which were available during the time of thesis writing, were overweight for a femtosatellite. Therefore with this enhancement, a femtosatellite can achieve active control over the satellite rather than passive if this light-weight technology is achieved.

The structure of this femtosatellite can be improved from the rectangular stack to a modular structure to save more space and mass than this current model. The modular structure has to deal with the wiring problem that would arise due to the shape.

Different designs should be laid out to support different types of payloads other than a camera and sensors. It could, therefore, become more fruitful, and different types of functions and applications could be achieved.

13 Summary

The purpose of the thesis is to analyze the feasibility of a 100-gram femto class satellite. The reason behind this research is to find out, whether the femtosatellite is able to communicate in the form of sending and receiving images taken from the camera. The thesis is composed of thirteen chapters, each of which deals with different aspects of design for the femtosatellite.

Chapters One to Three are introductory and define basic terminologies, background, and goals described in the thesis, such as the Orbit of the satellite, the weight limit for the satellite and these first three chapters describes previous works on femtosatellites.

Chapter One is subdivided into two parts. Chapter One describes the introduction, goals, and classes of femtosatellites and the motivation for it is mentioned in its sub-chapter. The Background study of femtosatellites and previous literature on this project is explained in Chapter Two.

The third chapter describes the methodology of this project and how to complete this project in different phases. From Chapter Four onwards till Chapter Ten, the subsystems of the femtosatellite are described. Chapters Two to Seven are primary subsystems of the satellite.

The power subsystem of the femtosatellite is examined in Chapter 4, and previous works on this subsystem are briefly discussed. The chapter consists of three parts: the Solar panels, charge controller, and battery.

The communication Subsystem is focused on in Chapters Five and Six. The antenna and its making process in CST are described in Chapter 5 while different parts of communication such as the link budget, transceiver, PA, and LNA are explained in Chapter Six. The attitude control system of the femtosatellite is investigated in Chapter Seven. Literature is presented at the start and the actual design at the end.

The operational part of the femtosatellite is described in Chapters Eight to Eleven. The structure of the femtosatellite is briefed and starts from the available structure in the market and ends up in defining a structure based commercial available parts.

The approach towards the payload is illustrated in Chapter Nine. Previous studies, such as in the other chapters, are mentioned at the start, and then the commercially-made model in its subheadings is presented at the end. Chapter Ten is about the OBC and looks at different types and the OBCs and presents its model in its subsections.

Lastly, the internal design of the femtosatellite functionality is described in Chapter Eleven. It has three subheadings which are the block diagram, the schematic and the mass and power budget.

The conclusions resulting from the design of the femtosatellite are drawn in Chapter Twelve. It has two parts, the design that was made, and its features and challenges are presented in its first part, which was project introspect. Changes to be made in the design for the future work of the project are recommended in the second part.

References

[1] C. Cofield. (2016, september) Communication satellite lost in spacex rocket explosion was co-leased by facebook. Accessed 27.09.2017. [Online]. Available: http://www.space.com/33937-facebook-satellite-lost-in-spacex-rocket-explosion.html

[2] T. T. GROUP. (2015, september) State of the satellite industry report. Accessed 27.09.2017. [Online]. Available: http://www.sia.org/wp-content/uploads/2015/06/Mktg15-SSIR-2015-FINAL-Compressed.pdf

[3] J. Tristancho Martínez, "Implementation of a femto-satellite and a mini-launcher for the n prize," Master's thesis, Universitat Politècnica de Catalunya, 2010.

[4] Q. Project. (2017, june) Qb50. Accessed 27.09.2017. [Online]. Available: https://www.qb50.eu/index.php/project-description-obj

[5] S. Janson and D. Barnhart, "The next little thing: Femtosatellites," 2013.

[6] A. Becena, M. Diaz, and J. Cristobal Zagal, "Feasibility study of using a small satellite constellation to forecast, monitor and mitigate natural and man-made disasters in chile and similar developing countries," 2012.

[7] "Satellite drag," satellite Drag | NOAA / NWS Space Weather Prediction Center. [Online]. Available: http://www.swpc.noaa.gov/impacts/satellite-drag#/

[8] J. Halpine, S. Liu, E. Simburger, H. Yoo, D. Hinckley, and D. Rumsey, "Pico-satellite solar cell testbed qualification testing," in *2006 IEEE 4th World Conference on Photovoltaic Energy Conference*, vol. 2, May 2006, pp. 1975–1978.

[9] The.Economist.Newspaper.Limited. (2017, june) Technology quarterly, a sudden light. Accessed 27.09.2017. [Online]. Available: http://www.economist.com/technology-quarterly/2016-25-08/space-2016

[10] D. J. Barnhart, T. Vladimirova, and M. N. Sweeting, "Design of self-powered wireless system-on-a-chip sensor nodes for hostile environments," in *Circuits and Systems, 2008. ISCAS 2008. IEEE International Symposium on.* IEEE, 2008, pp. 824–827.

[11] KK. (2012, September) Homemade space satellites. Accessed 27.09.2017. [Online]. Available: http://kk.org/cooltools/diy-satellite-platforms/

[12] N. Tahri, C. Hamrouni, and A. M. Alimi, "Study of current femto-satellite approches and services," *International Journal of Advanced Computer Science and Applications*, vol. 4, no. 5, 2013.

[13] D. Barnhart, T. Vladimirova, A. Baker, and M. Sweeting, "A low-cost femtosatellite to enable distributed space missions," vol. 64, pp. 1123–1143, 06 2009.

[14] S. Seckel. (2016) The next big thing in space is really, really small. Accessed 27.09.2017. [Online]. Available: http://asunow.asu.edu/20160406-creativity-asu-suncube-femtosat-space-exploration-for-everyone/

[15] A. K. Maini and V. Agrawal, *Satellite technology: principles and applications*. John Wiley & Sons, 2011.

[16] S. F. D. S. (SFDS). (2017) Suncube. Accessed 27.09.2017. [Online]. Available: http://femtosat.asu.edu/suncube_femtosat_design_specifications_v1.pdf

[17] V. Agrawal, *Satellite Technology: Principles and Applications*. John Wiley & Sons, 2010.

[18] *NON-ISOLATED SWITCHING REGULATOR*, CUIINC, 4 2017, accessed 27.09.2017. [Online]. Available: http://www.cui.com/product/resource/p7805-s.pdf/

[19] P. Fortescue, G. Swinerd, and J. Stark, *Spacecraft systems engineering*. John Wiley & Sons, 2003.

[20] *Triangular Advanced Solar Cells (TASC)*, Spectrolab, 10 2002, accessed 27.09.2017. [Online]. Available: http://www.spectrolab.com/DataSheets/PV/PV_NM_TASC_ITJ.pdf

[21] *CTJ Photovoltaic Cell*, Solaero technologies, 3 2015, accessed 27.09.2017. [Online]. Available: http://solaerotech.com/wp-content/uploads/2015/03/CTJ-Datasheet.pdf

[22] M. Osborne, "Sharp launches high-efficiency mono back-contact 48-cell pv module," PV Tech Website, https://www.pv-tech.org/products/sharp-launches-high-efficiency-mono-back-contact-48-cell-pv-module.

[23] *30 % Triple Junction GaAs Solar Cell*, AZURSPACE, 4 2017, accessed 04.2017. [Online]. Available: http://www.azurspace.com/images/products/0004148-00-01_DB_GBK_80%\C2%\B5m.pdf/

[24] (2017, May) Space solar cells. Accessed 27.09.2017. [Online]. Available: http://www.azurspace.com/index.php/en/products/products-space/space-solar-cells

[25] "Sunny buddy solar charger," accessed 02.02.18. [Online]. Available: https://learn.sparkfun.com/tutorials/sunny-buddy-solar-charger-v13-hookup-guide-

[26] J. Hemmo, "Electrical power systems for finnish nanosatellites," 2013.

[27] (2017, May) Adafruit battery. Accessed 27.09.2017. [Online]. Available: https://www.adafruit.com/product/258

[28] K. Zenger, "Integration of a gps subsystem into the aalto-1 nanosatellite," Ph.D. dissertation, Aalto University, 2013.

[29] M. Mahmoud, "Integrated solar panel antennas for small satellites," 2009.

[30] M. W. Majeed, A. Khan, A. U. Rehman, and K. Rashid, "Microstrip patch antennas for microwave s band, c band and x band applications," *Bahria University Journal of Information & Communication Technology*, vol. 4, no. 1, p. 36, 2011.

[31] Q.-Q. He, B.-Z. Wang, and J. He, "Wideband and dual-band design of a printed dipole antenna," *IEEE Antennas and Wireless Propagation Letters*, vol. 7, pp. 1–4, 2008.

[32] Y. Liu, X. Guo, S. Gu, and X. Zhao, "Zero index metamaterial for designing high-gain patch antenna," *International Journal of Antennas and Propagation*, vol. 2013, 2013.

[33] J. Ung and T. Karacolak, "A cpw-fed rectangular slot antenna for s and c band applications," *Microwave and Optical Technology Letters*, vol. 55, no. 8, pp. 1714–1717, 2013.

[34] C. Kakoyiannis and P. Constantinou, *Electrically small microstrip antennas targeting miniaturized satellites: the cubesat paradigm.* INTECH Open Access Publisher, 2011.

[35] E. Fernandez-Murcia, L. Izquierdo, and J. Tristancho, "A synthetic aperture antenna for femto-satellites based on commercial-of-the-shelf," in *Digital Avionics Systems Conference (DASC), 2011 IEEE/AIAA 30th.* IEEE, 2011, pp. 8A3–1.

[36] R. Patil and S. Popalghat, "A review of various types of patch antenna."

[37] C. A. Balanis, *Antenna theory: analysis and design.* John Wiley & Sons, 2016.

[38] R. Waterhouse, *Microstrip patch antennas: a designer's guide.* Springer Science & Business Media, 2013.

[39] J. S. Roy and B. Jecko, "Simplified design theory for a circular microstrip patch antenna," *Microwave and Optical Technology Letters*, vol. 6, no. 3, pp. 201–205, 1993.

[40] C. A. Balanis, "Antenna theory: A review," *Proceedings of the IEEE*, vol. 80, no. 1, pp. 7–23, 1992.

[41] D. Barnhart, T. Vladimirova, and M. Sweeting, "Satellite-on-a-chip: A feasibility study," *Proc. 5th Round Table on Micro/Nano Technologies for Space," Nordwijk, The Netherlands*, 2005.

[42] J. S. Harris, "Analysis and implementation of communications systems for small satellite missions," 2016.

[43] J. Jussila *et al.*, "Aalto-1 nanosatelliitin s-kaistan lähetin," 2013.

[44] V. Antti and A. Lehto, *Radio engineering for wireless communication and sensor applications*. Artech House, 2003.

[45] G. Kennedy and B. Davis, *Electronic communication systems*, 4th ed. McGraw-Hill Publishing Co. Ltd, . ISBN 0-07-112672-4., p 509, 1992.

[46] *Single Chip 2.4GHz Transceiver*, NORDIC SEMICONDUCTOR, 4 2017, accessed 04.2017. [Online]. Available: http://www.solar-mems.com/smt_pdf/Brochure_NanoSSOC-A60.pdf/

[47] *Low-Cost Low-Power 2.4 GHz RF Transceiver*, Texas Instruments, 8 2017, accessed 27.09.2017. [Online]. Available: http://www.ti.com/product/CC2500

[48] *Wi-Fi Power Amplifier*, Qorvo, 5 2017, accessed 27.09.2017. [Online]. Available: https://www.qorvo.com/products/p/QPA5219

[49] *2.4-2.5 WLAN Low-Noise Power Amplifier*, MICROCHIP, 5 2017, accessed 27.09.2017. [Online]. Available: http://ww1.microchip.com/downloads/en/DeviceDoc/70005083B.pdf

[50] B. O. Takase, "Novel antenna technologies for small-satellite and terestrial applications," Ph.D. dissertation, 2008.

[51] A. Siahpush and J. Gleave, "A brief survey of attitude control systems for small satellites using momentum concepts," 1988.

[52] J. Carroll and J. Oldson, "Tethers for small satellite applications," 1995.

[53] M. Post, R. Bauer, J. Li, and R. Lee, "Study for femto satellites using micro control moment gyroscope," in *Aerospace Conference, 2016 IEEE*. IEEE, 2016, pp. 1–8.

[54] Z. Ding, J. Yuan, G. Lu, Y. Li, and X. Long, "Three-axis atomic magnetometer employing longitudinal field modulation," *IEEE Photonics Journal*, vol. PP, no. 99, pp. 1–1, 2017.

[55] L. Richard, "A three axis magnetometer for use in a small satellite," in *Applied Electronics, 2006. AE 2006. International Conference on*. IEEE, 2006, pp. 113–116.

[56] *Sun Sensor for Nano-Satellites Analog Interface*, SOLARMEMS technologies, 4 2017, accessed 27.09.2017. [Online]. Available: http://www.solar-mems.com/smt_pdf/Brochure_NanoSSOC-A60.pdf/

[57] *Ultralow Noise, Dual-Axis MEMS Gyroscope*, ANALOG DEVICES, 3 2014, accessed 27.09.2017. [Online]. Available: http://www.analog.com/media/en/technical-documentation/data-sheets/ADXRS290.pdf

[58] K. World Data Center for Geomagnetism, “Model field at a point by igrf (igrf-12),” Data Analysis Center for Geomagnetism and Space Magnetism Graduate School of Science, Kyoto University Kitashirakawa-Oiwake Cho, Sakyo-ku, http://wdc.kugi.kyoto-u.ac.jp/igrf/point/index.html.

[59] Supermagnete, “Disc magnet Ø 15 mm, height 8 mm,” Supermagnete, accessed 27.09.2017. [Online]. Available: https://www.supermagnete.de/eng/disc-magnets-neodymium/disc-magnet-diameter-15mm-height-8mm-neodymium-n42-nickel-plated_S-15-08-N

[60] E. S. Agency, “On board computer and handling,” 5 2014, accessed 27.09.2017. [Online]. Available: http://www.esa.int/Our_Activities/Space_Engineering_Technology/Onboard_Computer_and_Data_Handling/Onboard_Computers

[61] J. Eickhoff, *Onboard Computers, Onboard Software and Satellite Operations: An Introduction*. Springer Science & Business Media, 2011.

[62] H. Grobler, “Aspects affecting the design of a low earth orbit satellite on-board computer,” Ph.D. dissertation, Stellenbosch: Stellenbosch University, 2000.

[63] (2017, April) Raspberry-pi-zero. Accessed 27.09.2017. [Online]. Available: http://www.Raspberrypi.org/blog/Raspberry-pi-zero/

[64] (2017, April) Pinout! Accessed 27.09.2017. [Online]. Available: http://pinout.xyz/

[65] M. M. Verstraete, “Comment on "can you describe the payload of an earth observation satellite", researchgate website,” june 2015, accessed 27.09.2017. [Online]. Available: "https://www.researchgate.net/post/Can_you_describe_the_payload_of_an_earth_observation_satellite"

[66] M. Abolghasemi and D. Abbasi-Moghadam, “Conceptual design of remote sensing satellites based on statistical analysis and niirs criterion,” *Opt. Quant. Electron*, 2015.

[67] dagorym (https://physics.stackexchange.com/users/335/dagorym), “Cameras in voyager probes,” Physics Stack Exchange, uRL:https://physics.stackexchange.com/q/25007 (version: 2011-06-12). [Online]. Available: https://physics.stackexchange.com/q/25007

[68] S. B. U. K. Pimoroni Ltd. 2 Manton Street, Sheffield, “Raspberry pi camera v2.1 with mount,” Pimoroni, tech treasure for tinkers, uRL:https://shop.pimoroni.com/products/Raspberry-pi-camera-module-v2-1-with-mount (version: 2017-07-10). [Online]. Available: https://shop.pimoroni.com/products/Raspberry-pi-camera-module-v2-1-with-mount

[69] (2017, june) Pi foundation raspberry pi zero case + mini camera cable. Accessed 27.09.2017. [Online]. Available: https://www.adafruit.com/product/3446

[70] K. Marjoniemi, L. Syvonen, M. Hoffren, and S. Langois, "Modular structure for small satellites," in *Small Satellites, Systems and Services*, vol. 571, 2004.

[71] G. Steve Price, Dr. Tony Phillips. (2001, March) Staying cool on the iss. Accessed 27.09.2017. [Online]. Available: https://science.nasa.gov/science-news/science-at-nasa/2001/ast21mar_1